12-2015

Computer Aided Brain Tumor Edge Extraction Using Morphological Operations

Warqaa Shaher AlAzawee

COMPUTER AIDED BRAIN TUMOR EDGE EXTRACTION USING MORPHOLOGICAL OPERATIONS

by

Warqaa Shaher AlAzawee

A thesis submitted to the Graduate College
in partial fulfillment of the requirements
for the degree of Master of Science in Engineering (Computer)
Department of Electrical and Computer Engineering
Western Michigan University
December 2015

Thesis Committee:

Dr. Ikhlas Abdel Qader, Ph.D., Chair
Dr. Raghvendra Gejji, Ph.D.
Dr. Jareer Abdel Qader, Ph.D.

COMPUTER AIDED BRAIN TUMOR EDGE EXTRACTION USING MORPHOLOGICAL OPERATIONS

Warqaa Shaher AlAzawee, M.S.E.

Western Michigan University, 2015

Detecting the precise boundary of the area containing a recognized brain tumor is a complex problem and must be addressed since it applies to many medical modalities and tumor types. The objective of this thesis is to provide an efficient algorithm for detecting edges of brain tumors to help neurosurgeons identify the border of the critical area and distinguish the precise margin of the tumor from the rest of the brain tissue during the surgery. This thesis work exploits MRI brain tumor images as a tool to aid surgeons. MRI image segmentation is an essential step as a preliminary process to localize the region of interest, which is the brain tumor region. This work proposes a new method using morphological operators and utilizing an erosion process to identify and extract the boundary of a brain tumor. Using abnormal images of a variety of brain tumors, this study shows that the proposed algorithm provides a robust method in terms of accuracy and computation time, making it suitable for real-time processing. Results also show that this algorithm is capable of producing one-pixel-width continuous edges as well as accurate positioning of abnormal cells. This study also presents the results of a comparative study of its proposed method and common edge detection techniques such as Sobel, Robert, Prewitt, Canny and Cellular Automata.

ACKNOWLEGMENTS

There are many people to whom I owe a debt of thanks for their support over the last two years. First, I would like to express my gratitude, appreciation and thanks to my advisor Dr. Ikhlas Abdel Qader for her support, guidance and encouragement in completion of this thesis. She always found adequate time to oversee my studies and share her knowledge and expertise with me. She stood by not only as a supervisor but also as a big sister. I would also like to express my sincere appreciation to my committee member Dr. Jareer Abdel Qader for his support and time in the preparation of this work. Moreover, I would like to thank Dr. Raghvendra Gejji for his support as my committee member.

I would like to express special thanks to my family for their invaluable support and guidance throughout my life. A special feeling of gratitude is directed towards my loving parents, Shaher AlAzawee and Zakia Hassuny whose words of encouragement and push for tenacity ring in my ears. My sister and my brothers have never left my side and are very special.

Above all, I owe my deepest gratitude and special thanks to my beloved, incredibly wonderful husband, Ahmed Altaie, and my beautiful and precious children Massarra, Yman, and Yousef. Thank you for your love, support, patience, and numerous sacrifices throughout my academic program. I love each one of you more than I can say. This thesis and the pursuit of my goals would not have been possible without you.

Warqaa Shaher AlAzawee

TABLE OF CONTENTS

Table of Contents - Continued

Table of Contents - Continued

LIST OF TABLES

LIST OF FIGURES

List of Figures - continued

CHAPTER I

INTRODUCTION

1.1 Brain Tumor

The brain is the center of the nervous system, and it is the most complex organ in the human body. It is a non- replaceable and soft and spongy mass of tissue. Therefore, any damage or harm in the brain will cause problems for personal health including mobility or cognition [1-2]. The brain tumor is a group of abnormal cells that grows inside the brain or around the brain. A brain tumor does not only impact the immediate cells in its location but it also can cause damage to surrounding cells by causing inflammation. A malignant tumor, in addition to other cancerous growth, has several classifications such as astrocytoma, meningioma, glioma, medulloblastoma and metastatic as shown in Figure 1.1 [3]. These tumors are different in appearance, shape, size and location. Also, these tumors appear as either hypointense (darker than brain tissue), isointense (same intensity as brain tissue), or hyperintense (brighter than brain tissue) as shown in Figure 1.2 [3]. The tumor may be primary when it is at origin, while it will be classified as secondary when the part of tumor is spread to another place and grown on its own [1-2]. Surgery can be the recommended treatment in many cases such as the following:

- Surgery is essential when complete removal of is necessary as much as possible [1].

- Surgery for a brain tumor may be recommended to provide a tumor tissue sample for an accurate diagnosis [1].
- Surgery is often required to remove at least some part of the tumor to relieve pressure inside the skull (intracranial pressure), or to reduce the amount of tumor to be treated with radiation or chemotherapy [1].
- Surgery for a brain tumor is recommended to relieve seizures (due to a brain tumor) that are difficult to control with other means [1].
- Surgery for a brain tumor is recommended to enable direct access for chemotherapy, radiation implants or genetic treatment of a malignant tumor [1].

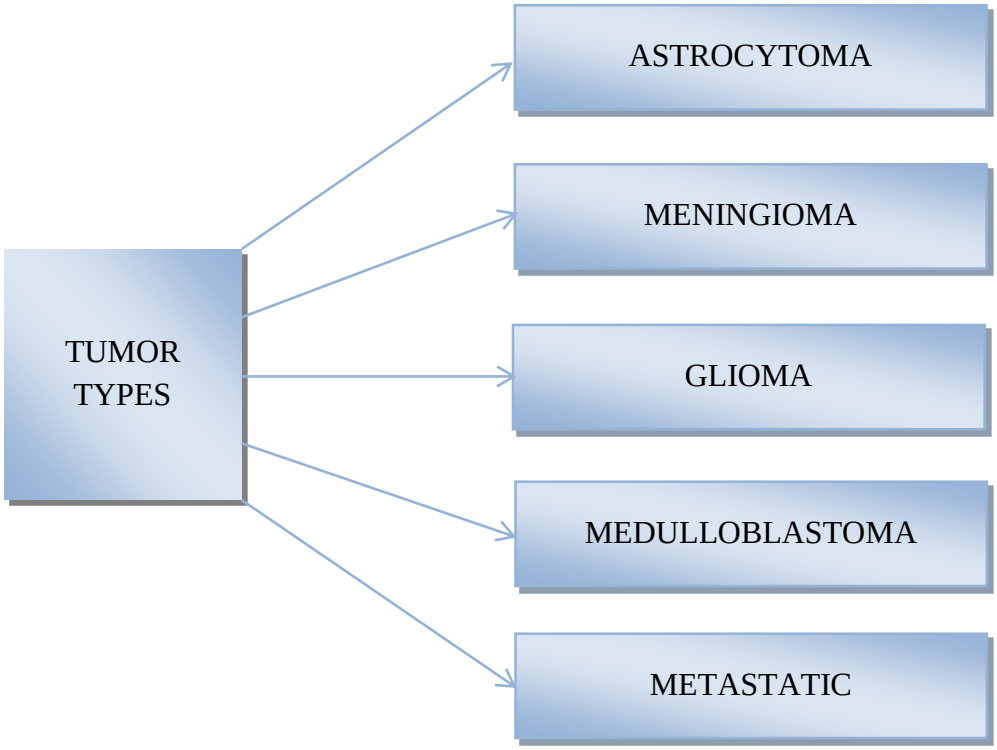

Figure 1-1: Types of Brain Tumor [3].

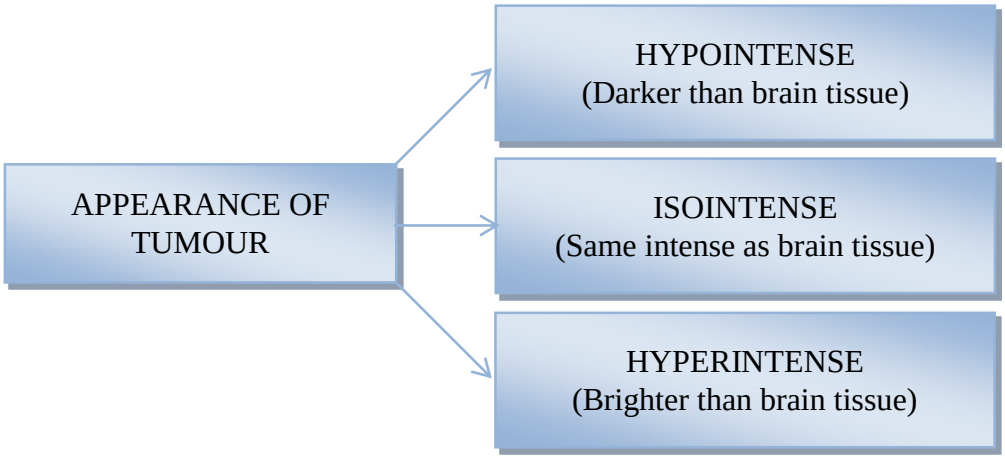

Figure 1-2: Appearance of Brain Tumor [3].

Neurosurgeons use as many tools as they can when trying to remove a brain tumor. Brain Mapping is used during surgery to help the neurosurgeon detect critical areas and distinguish the margins of the tumor from the rest of the brain tissue [1]. Brain mapping tools include the following:

1. Direct cortical stimulation: these techniques identify sensitive areas of the brain through direct contact with brain tissue. A probe is used to stimulate certain areas of the brain with a low dose of electrical current. This helps the neurosurgeon identify critical areas of the brain that must be carefully navigated [1].

2. Somatosensory-Evoked potentials (SSEP): low doses of electrical current are given to a limb or the face. Electrodes placed on the surface of the brain record the weak electrical impulses as they travel along nerves to the brain. It is another tool for identifying critical areas [1].

3. Functional MRI (fMRI): It is a scanning technique that takes faster images of the brain than traditional MRIs and creates pictures of the brain's use of oxygen. Consequently, this helps to distinguish between a normal brain, which uses oxygen, and a tumor that contains dead cells that do not use oxygen. It may be referred to as real time MRI, fast MRI or dynamic MRI [1].

4. Intraoperative Ultrasound Imaging: This technique is used during surgery, Ultrasonic waves are used to determine the depth of the brain tumor and its size. It works by sending ultrasonic pulses into brain, and these pulses then are reflected back. The time it takes is calculated by a computer and formed into an image on a screen. These images can help the neurosurgeon because they determine the shortest surgical rout to the tumor, they define the borders of the tumor, and they distinguish the tumor from swelling and a normal brain [1].

5. Intraoperative MRI (iMRI): Some operating rooms have specialized MRI machines that allow scans to be performed during surgery. These images provide the surgeon with information similar to an intraoperative Ultrasound, but they usually produce a more detailed image; they are particularly helpful in determining how much of the tumor has been removed and allow the surgeon to navigate using updated brain images [1]. Although once available at only a few centers, iMRI is now more widely available [1].

1.2 Problem Statement and Significance

As stated in a recent fact sheet published by the United States' Central Brain Tumor Registry (CBTRUS) in 2014, the incidence rate of all primary malignant and non-malignant brain and CNS tumors is 21.42 cases per 100,000 for a total count of 343,175 incident tumors; (7.25 per 100,000 for malignant tumors for a total count of 115,799 incident tumors and 14.17 per 100,000 for non-malignant tumors for a total count of 227,376 incident tumors) [4]. In addition, an estimated 68,470 new cases of primary malignant and non-malignant brain and CNS tumors are expected to be diagnosed in the United States in 2015. This includes an estimated 23,180 primary malignant and 45,300 non-malignant tumors expected to be diagnosed in the US in 2015 [4]. A brain tumor is an awful disease, and a surgery is one of the treatment methods. Image-guided surgery (IGS) is taking its path in brain tumor surgeries due to the sensitivity of brain cells and the impact of any unneeded loss of healthy brain cells or tissue [5]. Imaging technologies for surgeries include mapping and planning subsystems, navigational tools, and imaging devices used during surgery to provide neurosurgeons with the best informative status and location of the tumor during a biopsy or surgery. However, one of the biggest concerns when removing brain tumors is the possible loss of brain function afterward, which is why doctors are very careful to remove only as much tissue as is safely possible [6]. This thesis approaches edge detection as a tool to precisely identify the tumor edges from MRI images. This paper will focus on MRI images because the MRI scan doesn't

affect the human body, it doesn't use any radiation, and it is more comfortable as compared to a CT scan for diagnosis [3] [7].

1.3 Magnetic Resonance Imaging (MRI)

An MRI system uses superconducting magnets to provide a strong uniform steady magnetic field. It is unclear magnetic resonance imaging (MRI), or magnetic resonance tomography (MRI) [8]. MRI is used to distinguish pathologic tissue (such as a brain tumor) from normal tissue. The patient lies within a large powerful magnet. The magnetic field is used to align the magnetization of some atomic nuclei in the body, and then frequency fields systematically alter the alignment of this magnetization. This magnetic field is controlled by computer, and the received nuclear magnetic resonance signal is picked up by the receiver coil and fed into the receiver for signal processing. Also, images are constructed by the computer and analyzed by applying suitable image processing techniques [8]. This process will produce accurate and detailed pictures of organs from different angles to diagnose any abnormalities. Furthermore, MRI images allow the physician to vision even hairline cracks and tears in injuries to ligaments, muscles and other soft tissues. On the other hand, MRI has advantage; an MRI scanner is harmless to patients because it uses strong magnetic fields and non-ionizing electromagnetic fields in the radio frequency range. Therefore, it is unlike CT scanners and traditional X-rays [3]. The two most commonly used MRI visualizations are T1-weighted and T2-weighted images. These weightings point out to the dominant signal (whether it be the T1 time or the T2 time) measured to produce the contrast observed in

the image. The areas with high fat content have a short T1 time relative to water; T1-weighted images can be thought of as visualizing locations of fat [10]. High-fat-content tissues appear as bright areas of high signal intensity, while High-water-content tissues appear as dark areas of low signal intensity [3] [9]. In contrast, the areas with high water content have a short T2 time relative to areas of high fat content, T2-weighted images can be thought of as visualizing locations of water [10]. High-fat-content tissues appear as dark areas of high signal intensity, while High-water-content tissues appear as bright areas of low signal intensity [3] [9]. Figure 1.3 shows an example T1- and T2-weighted image and the locations of two normal tissue types in these modalities. Most brain tumors have tissue that contains water. Therefore, brain Tumors will be white in T2 and black in T1 [9]. For visualizing brain tumors in T1, a second T1-weighted image is often acquired after the injection of a 'contrast agent'. These 'contrast agent' compounds usually contain an element whose composition causes a decrease in the T1 time of nearby tissue (gadolinium is one example) [10-9]. Figure 1.4 illustrates a T1-weighted image before and after the injection of a contrast agent. Brain tumors in a T1-weighted image after the injection of a contrast agent appear as bright regions [9-10]. The presence of this type of 'enhancing' area can indicate the existence of a tumor, and can be a strong indicator of tumor location [10]. Generally, an MRI has the ability to distinguish the differences between two arbitrarily similar but not identical tissues. In relation to this thesis, MRI images are essential to identify a brain tumor.

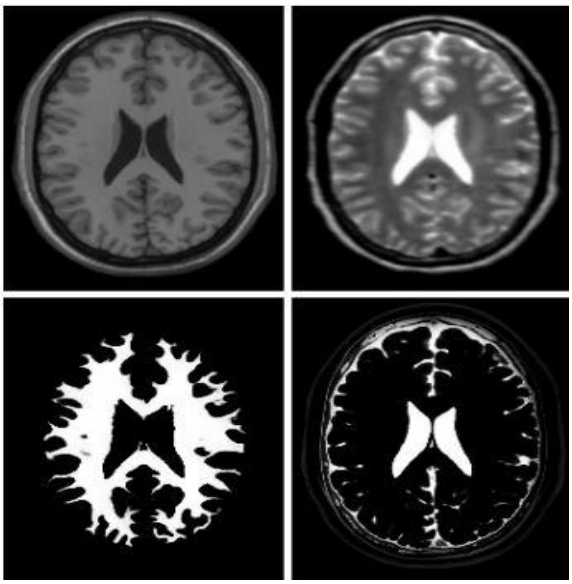

Figure 1-3: T1-Weighted And T2-Weighted Signal Properties. Top Left: T1-Weighted Image (Light Regions Visualize Locations of Fat). Top Right: T2-Weighted Image (Light Regions Visualize Locations of Water). Bottom Left: White Matter (High Fat) Locations. Bottom Right: Cerebrospinal Fluid (High Water) Locations [10].

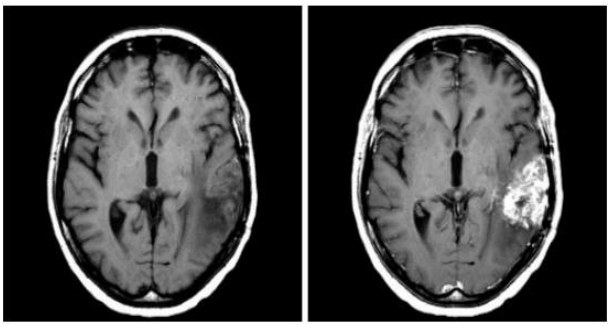

Figure 1-4: Effects of Contrast Agent on T1-Weighted Image Data. Left: T1-Weighted Image Prior To the Injection of a Contrast Agent. Right: T1-Weighted Image after the Injection of a Contrast Agent [10].

1.4 Research Goal and Proposed Methodology

This thesis aims to address brain tumor edge detection from MRI images to be used as a tool in real time during surgeries. The framework is based on image segmentation by using the thresholding technique. Otsu's thresholding technique has been adapted in this work. Then, a new method is proposed for edge detection using morphological operations and utilizing erosion processes to identify the edges of a brain tumor. Finally, the study applies different edge detection techniques including Roberts, Prewitt, Sobel, Canny Operator, and Edge detection based on Cellular Automata to investigate the best performing edge detector in terms of accuracy and complexity. This framework is presented also in Figure 1.5.

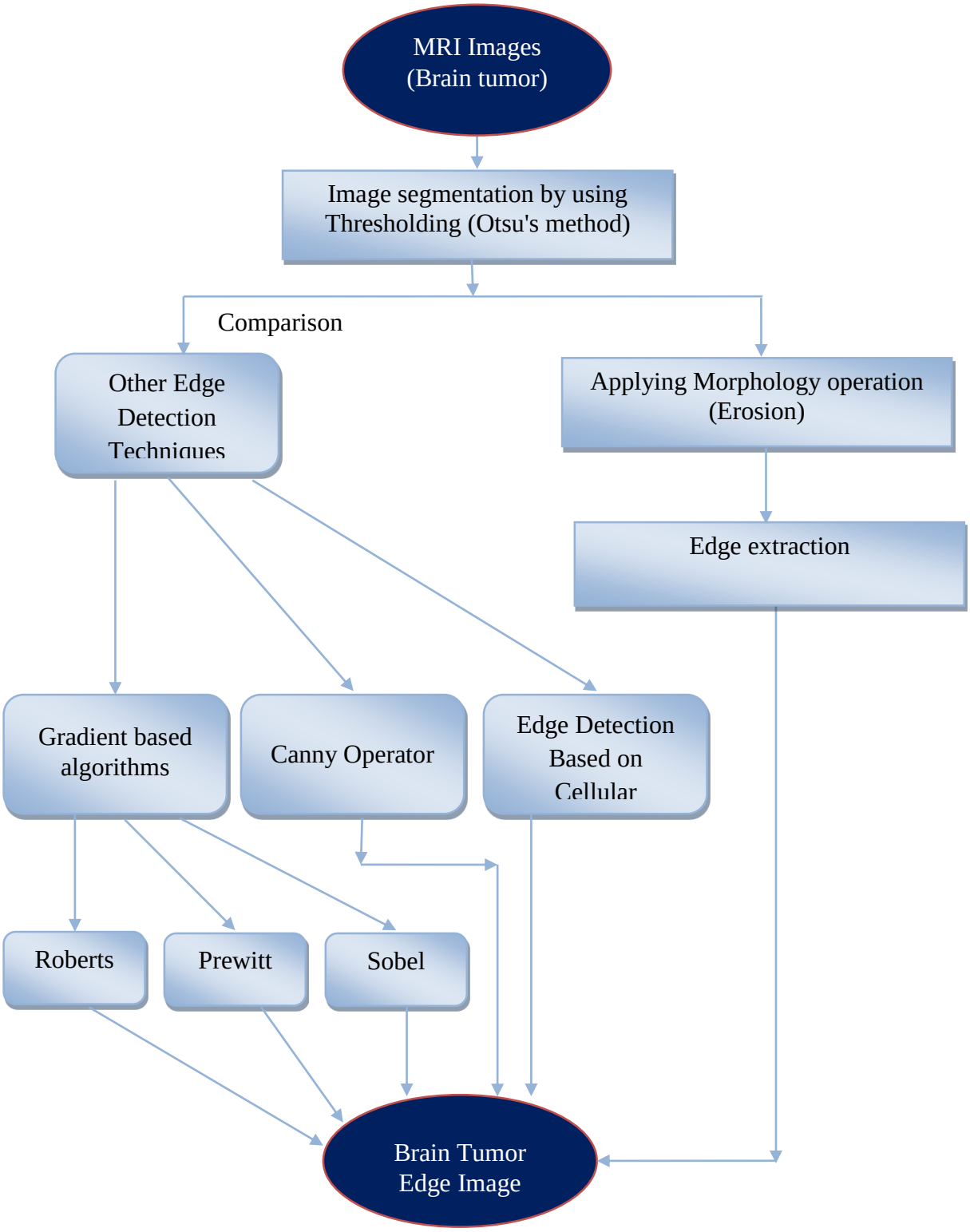

Figure 1-5: The Proposed Work.

1.5 Related Work

Numerous methods have been proposed to address the need for better edge detection methods to address brain tumor MRI images and to be used as a tool in real time during surgeries. Recently, Aysha Bava M et al. (2014) studied segmentation of a brain tumor in MRI using Multi-structural Element morphological edge detection. In their research, a morphological edge has been found using the opening and closing operations. Their results showed that their algorithm is more efficient for medical image analysis and edge detection than the usual edge detection methods such as Sobel, Prewitt, Robert and Canny edge detector. However, its computation is more complex compared to these conventional edge detection techniques [11].

Pratibha Sharma et al. (2012) studied an application of edge detection for brain tumor detection. Their algorithm involved various steps. They used a Median filter to remove noise and a Laplacian filter. Then, they converted the image to binary and applied morphological operations (erosion and dilation) to smooth results. Finally, for edge detection, they used the 2D cellular automata rule 255. Also, they used Watershed segmentation as a method for verifying output. Their algorithm was applied on numerous images, and the results were good. However, accuracy obtained in the final result depends on processing of each step. For each step, there are numerous methods available. Therefore, it is hard to choose the suitable methods that provide best results [12].

C.C. Leung et al. (2003) proposed a new approach to detect the boundary of a brain tumor based on the generalized Fuzzy operator (GFO). One typical example is used

for evaluating this method with the contour deformable model (CDM). Their result showed that the boundary detection using their method is better than the method of CDM. However, there is a 2% error in their method because there is a small region of normal tissue located within the tumor. As a result, their method remains inefficient to detect the boundary for the brain tumor [13].

Riries Rulaningtyas et al. (2009) studied edge detection for brain tumor pattern recognition. In their research, they enhanced the image using a histogram. Then, they used an edge detection process to take the edge pattern of a brain tumor. They used three methods of edge detection (Robert, Prewitt, and Sobel). The obtained results showed that Sobel is more suitable for edge detection of a brain tumor than the Robert and Prewitt operators [14].

Manoj Diwaker et al. (2013) proposed a new method for edge detection using cellular automata. They used Cellular Automata rules to help determine the exact location and size of a brain tumor. They adopted Cellular Automata rule 124 in their research. Also, they presented comparison results between their method and Sobel, Robert, Prewitt, Canny and Marr-Hildreth methods. Their results showed that the output obtained by Cellular automata is better than conventional methods [15].

Nassir Salman (2006) suggested Image segmentation and edge detection based on the Chas-Vese algorithm. Salman used K-means to detect regions in a given image. Then, based on techniques of curve evaluation, Chan-Vese for segmentation and level sets approaches detect the edges around each selected region. He obtained a segmented image with a closed boundary per one actual region. The accuracy of his results for edge

position and region segmentation have been compared with active contours without edges and image segmentation and edge detection based on the watershed technique. He found that his image has better region segmentation and edge detection results. However, the amount of iteration in his algorithm is large and time consuming. Also, the accuracy of his results for edge position depends on the fact that if the result of k-means are accurate then the regions boundaries are in correct positions [16].

Ali S.M. et al. (2013) studied brain tumor extraction in MRI images using clustering and morphological operations techniques. In their research, MRI T2 weighted modality has been preprocessed by a bilateral filter to reduce the noise and maintain edges among the different tissues. They used the morphological operation (erosion and dilation) to smooth four different techniques: Gray level stretching and Sobel edge detection, the K-means clustering technique based on location and intensity, the Fuzzy C-means clustering, and an Adapted K- means technique. Their results showed that the four implemented techniques can successfully detect and extract the brain tumor. However, more work is required to improve the segmentation results, and this may be achieved by implementing certain supervised classification methods [17].

Hemang J. Shah (2014) proposed in his paper a hybrid approach, which is a combination of the watershed method and the canny edge detection method to detect the tumor boundaries in an MRI image for different cases of brain tumor. The result showed that this combination can be used; it provides effective extraction of a tumor in MRI images and also enhances the performance of the watershed method [18].

Hemang J. Shah et al. (2014) studied various methods for detecting a tumor on MRI Images. In their research, they compared different image segmentation methods for evaluating their performance in the segmentation of a tumor. Those were Level Set Segmentation, K-means clustering, Difference in Strength Technique, and Watershed method. From their results, they concluded that all these methods have their own advantages and disadvantages. Level Set Segmentation requires the prior choice of the critical parameters such as the initial location of seed point, the appropriate propagation speed function and the degree of smoothness. The output image from K-means clustering has different intensity regions. An incorrect choice of threshold results in very weak accuracy in the segmented image when using Difference in Strength technique. Finally, Watershed suffers from the problem of over segmentation (a large number of segmented regions around each local minimum in the image) [19].

Work by Rachana Rana et al. (2013) presents various methods for brain tumor segmentation for MRI images. These were seed-based regions growing, Level-set segmentation, Graph- based segmentation, Split and Merge-based segmentation, Edge based segmentation, and Morphological operations. In their research, they concluded that, in spite of the availability of a large variety of state-of art methods for brain MRI segmentation, it is still a tough task, and there is a need and wide scope for future research to improve the precision and accuracy of segmentation methods. Introducing new methods and combining different methods can be future schema for making improved brain segmentation methods [3].

In all, the proposed algorithms are suffering from disadvantages in terms of accuracy and computation time. Due to these various disadvantages, this thesis aims to produce an effective edge detection method, which will overcome of these disadvantages.

1.6 Thesis Outline

This thesis is structured in five chapters, including this introduction. These chapters consist of the following:

Chapter 1 provides a definition of a brain tumor and the popular techniques that are used during surgery to remove the brain tumor. Also, it provides related works that researchers have done on this topic.

Chapter 2 provides the background of segmentation techniques and describes how the brain tumor area is extracted using Otsu's Thresholding technique.

Chapter 3 provides, for comparison, a review of other edge detection techniques that have been used.

Chapter 4 presents this thesis's proposed edge detection technique: to detect the edges of a brain tumor by morphological operations utilizing the Erosion concept.

Chapter 5 discusses and analyzes the results to prove that this thesis's proposed method provides a robust method in terms of accuracy and computation time.

Finally, Chapter 6 presents the conclusions and recommendations for further studies and research.

CHAPTER II

BRAIN TUMOR SEGMENTATION BY THRESHOLDING (OTSU'S METHOD)

2.1 Background (Segmentation Technique)

Segmentation refers to the segregation area of interest from the image. The main goal of image segmentation is to cluster the pixels into salient image regions. Segmentation also is used to simplify the representation of an image into something that is more meaningful and easier to analyze, and Image segmentation is used to locate objects and boundaries (lines, curves) in images [20]. Moreover, these regions are corresponding to individual surfaces, objects, or natural parts of objects. Also, segmentation should stop when the objects or regions of interest in an application have been detected. Most segmentation algorithms are based on one of two basic properties of intensity value: discontinuity and similarity. In addition, there are two approaches for the segmentation technique. The first approach is to partition an image based on abrupt changes in intensity, and the second approach is based on partitioning an image into regions that are similar according to a set of predefined criteria such as thresholding, region growing, region splitting and merging methods [20]. On the other hand, there are many of different applications for the segmentation technique, such as automatic car assembly in robotic vision, airport security systems, object recognition, criminal investigation, computer graphics, medical imaging and MPEG-4 video object (VO) segmentation [21]. In relation to this paper, the segmentation technique is one of the most important techniques in the medical field, especially for brain tumor detection and

extraction. It plays an important role in image processing for MRI images [22]. A significant medical informatics task is to perform the indexing of the patient databases according to image location, size, and other characteristics of a brain tumor based on MRI imagery [23]. However, brain tumor segmentation from MR modalities is considered a challenging and intensive task because MRI and medical images contain complicated anatomical structures that require precise and most accurate segmentation for clinical diagnosis [22]. Many people who had brain tumors died due to inaccurate detection and extraction [24]. Therefore, different segmentation algorithms are developed for this purpose. Despite the wide number of automatic image segmentation techniques that are used for brain tumor extraction , they fail in most cases largely because of unknown and irregular noise, inhomogeneity, poor contrast and weak boundaries which are ingrained in medical images [25]. The main challenges to any segmentation algorithm are the following:

- Noise
- The bias field (the presence of smoothly varying intensities inside tissues)
- The partial-volume effect (a voxel contributes in multiple tissue types)

Removing noise from MRI images is a preprocess step before applying any segmentation algorithm. However, accurate removal of noise from an MRI image is a challenge, and de-noising is still an open issue; de-noising methods need improvement. Nonlinear filtering methods and linear filters are used for removing noise. Linear filters are used to reduce noise by updating pixel value by the weighted average of a

neighborhood. However, these degrade the image quality substantially. On the other hand, there are different Nonlinear filtering methods, but these methods are almost identical in terms of computation cost, de-noising, quality of de-noising and boundary preserving. Also, these methods preserve edges but degrade fine structures. Some of these de-noising methods are a Markov random field method (MRF), Wavelet-based methods, the Analytical correction method, and the Non-local (NL) method [25].

2.1.1 Fundamentals of the Segmentation Technique

Let us suppose R represents the entire spatial region occupied by an image. Therefore, image segmentation can be viewed as a process that partition R into n sub regions such as R1, R2, R3 as shown in figure 2.1:

a. $\bigcup_{i=1}^{n} R_i = R$

b. R_i is a connected set, i=1,2,....,n.

c. $R_i \cup R_j = \emptyset$ for all i and j, $i \neq j$.

d. $Q(R_i)$ = TRUE for i= 1,2,.....n.

e. $Q(R_i \cup R_j)$= FALSE for any adjacent regions Ri and Rj.

Figure 2-1: The Process for How a Segmentation Technique Works.

From steps above, $Q(R_k)$ is a logical predicate defined over points in set R_k, and the null set is Ø. On the other hand, the symbol ∪ and ∩ represent sets union and intersection respectively. As a result the two regions R_i and R_j are said to be adjacent if

their union forms a connected set. However, condition (a) shows that the segmentation must be complete because every pixel must be in a region, while condition (b) indicates that the points in a region be connected in some predefined sense. For example, the points must be 4- or-8 connected. On the other hand, condition (c) shows that the regions must be disjointed, while the condition (d) indicates the properties that must be satisfied by the pixels in a segmentation region. Therefore, $Q(R_i)$ = TRUE if all pixels in R_i have the same intensity level. Eventually, the condition (e) shows how the two adjacent regions R_i and R_j must be different in the sense of predicate Q. Against this background, there is a fundamental problem in segmentation which is to partition an image into regions that satisfy the preceding conditions [20].

Finally, it is known that brain tumor detection is one of the challenging tasks in medical image processing. Consequently, there are different segmentation methods that have been used to identify, detect, and extract a brain tumor from MRI images. Some examples are the Fuzzy C-Mean Algorithm, K-Mean Clustering, a bounding box method, the Learning Vector Quantization (LVQ) method, the graph cut based method, the edge based segmentation method, the region growing method, the seed-based region growing method, level-set segmentation, and the Thresholding Method. Each one of these techniques has its own advantages and disadvantages. In this work, Otsu's Thresholding Method has been proposed to isolate a brain tumor from other regions of the brain images because it is the most suitable method [22]. It is compared with different standard segmentation techniques. The results showed that the degree of the accuracy of the

Otsu's method was 8.1, which is the highest value compared to other segmentation methods as shown in Table 2-1 [22]. Also, Otsu’s Thresholding has a significant level above 95% in both completeness and correctness of the segmented images [22].

Table 2-1

Results for Comparison of Common Image Segmentation Methods for Segmentation of Brain Tumors [22].

Segmentation Method	Degree of Accuracy of the Segmentation (out of 10)
Otsu's method	8.1
Mean Shift	6.1
K-means	6.0
Fuzzy c-means	5.2
Expectation maximization	4.5
Discrete Topological Derivative	4.2
Continuum Topological Derivative	3.9
Iterative Thresholding	3.8
Two Seed Region Growing	2.2
One Seed Region Growing	2.2

2.2 Image Segmentation Using Thresholding

In fact, the gray levels of pixels belonging to the object are quite different from the gray levels of the pixels belonging to the background in many applications of image processing. Therefore, the Thresholding technique becomes an effective tool to separate objects from the background. The output of the Thresholding operation is a binary image whose gray level of 1 (white) will indicate a pixel belonging to object and a gray level of 0 (black) will indicate the background [20]. As a result, image Thresholding enjoys a central spot and plays a vital role in applications in image segmentation because of its computational speed, its intuitive properties, and simplicity of implementation [20].

2.2.1 Fundamentals of the Thresholding Technique

Thresholding includes techniques for partitioning an image directly into regions based on intensity values and or properties of these values. Therefore, in the basics of intensity Thresholding, we suppose that the intensity histogram in Figure 2.2 corresponds to an image f(x,y). This image composed of light objects on a dark background. Therefore, in this way the object and background pixels will have intensity values grouped into two dominant modes. Now, it is possible to extract the objects from the background by selecting a threshold T. This threshold separates these modes. After that, any point (x,y) in the image is called an object when $f(x,y)>T$, while the point is called a background when $f(x,y)\leq T$ as shown in equation (2-1) [20].

$$g(x,y) = \begin{cases} \mathbf{1} & \mathbf{if\ f(x,y)\ > T} \\ \mathbf{0} & \mathbf{if\ f(x,y) \leq T} \end{cases} \quad (2\text{-}1)$$

When the value of T is a constant and applied over an entire image, this process is called global thresholding. On the other hand, when the value of T changes over an image, this process is called variable thresholding; this is where the value of T at any point (x,y) depends on properties of a neighborhood of (x,y) [20]. Also, the term local or regional thresholding is used to denote variable thresholding. This term also referred to as dynamic or adaptive thresholding since the value of T depends on the spatial coordinates (x,y) [20].

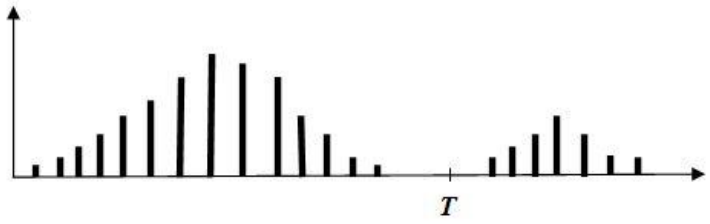

Figure 2-2: Intensity Histogram for an Image Composed of a Light Object on a Dark Background and How Global Thresholding (T) Is Applied Over an Entire Image.

Multiple thresholding is used when a histogram has more than two dominant modes. For example, an image has two types of a light object on a dark background as in the histogram in Figure 2.3. A point (x,y) belongs to one of these two objects if $\mathbf{T_1} < \boldsymbol{f(x,y)} \leq \mathbf{T_2}$, the other object class if $\boldsymbol{f(x,y)} > \boldsymbol{T_2}$, and a point (x,y) belongs to the background if $\boldsymbol{f(x,y)} \leq \boldsymbol{T_1}$ as shown in equation (2-2) [20].

$$g(x,y) = \begin{cases} \boldsymbol{a} & \mathbf{f(x,y)} > \boldsymbol{T_2} \\ \boldsymbol{b} & \boldsymbol{T_1} < \mathbf{f(x,y)} \leq \boldsymbol{T_2} \\ \boldsymbol{c} & \mathbf{f(x,y)} \leq \boldsymbol{T_1} \end{cases} \quad (2\text{-}2)$$

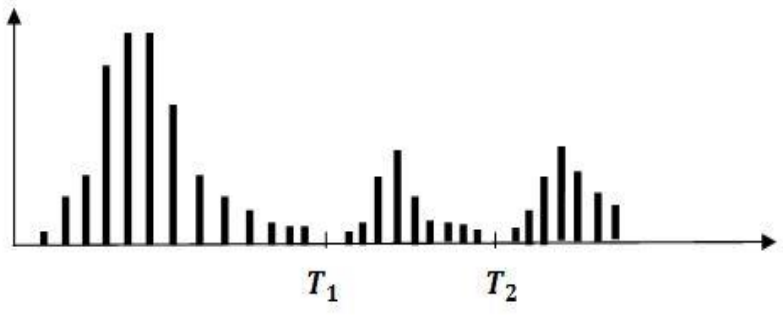

Figure 2-3: Intensity Histogram for an Image Composed of Two Types of Light Objects on a Dark Background and How Multiple Thresholding (T1, T2) Is Applied Over an Entire Image.

2.3 Segmentation Using the Basic Global Thresholding Method

This type of thresholding is simple because it is used when the intensity distribution of objects and background pixels are sufficiently distinct. It uses a single (global) threshold applicable over the entire image. An iterative algorithm can be used to automatically estimate the threshold value for each image required [27]. These are the following steps for this algorithm:

1. Select an initial estimate for the global threshold, T, which must be greater than the minimum and less than maximum intensity level in the image.
2. Segment the image using T; this process will produce two groups of pixels ($\boldsymbol{G_1}$) for all pixels $>$ T, and ($\boldsymbol{G_2}$) for all pixels $\leq$ T.
3. Compute the average (mean) intensity values $\boldsymbol{m_1}$ and $\boldsymbol{m_2}$ for the pixels in the two groups ($\boldsymbol{G_1}$) and ($\boldsymbol{G_2}$).

4. Compute a new threshold value: $\boldsymbol{T = \frac{1}{2}\ (m_1 + m_2)}$

5. Repeat steps 2 through 4 until the difference between values of T in succession are smaller than a predefined parameter $\boldsymbol{\Delta T}$ that is used to control the number of iteration in situations where speed is an important issue.

It works very well when there is a reasonably clear valley between the modes of the histogram related to objects and background [27].

2.4 Segmentation Using Otsu's Thresholding Method

This method is viewed as a statistical-decision theory problem with the objective of minimizing the average error incurred in assigning pixels to two or more groups [20]. These groups are called classes as well. Otsu's method is considered optimum because it maximizes between class variance [27] [20]. Also, it gives well-thresholded classes because these thresholded classes are distinct with respect to the intensity values of their pixels, and this thresholding gives the best separation between classes in term of their intensity values. In addition, this optimum method has the important property. This property is based entirely on computations performed on the histogram of an image [20].

As a result, we suppose {0, 1, 2, 3,....., L-1} when L distinct intensity levels in a digital image whose size is represented by M x N pixels, and let $\boldsymbol{n_i}$ denote the number of pixels with intensity i. In this method the normalized histogram is used because this method based on computation is performed on the histogram. So, the normalize histogram has components$\boldsymbol{p_{i=n_i/MN}}$, and its equation (2-3) is:

$$\sum_{i=0}^{L-1} p_i = 1, \qquad p_i \geq 0 \quad 1 \tag{2-3}$$

After that, we select a threshold T(k)=k, 0< k <L-1,and we will use it to threshold the input image into two classes which is C_1 and C_2. The C_1 class consists of all the pixels in the image with intensity values in rang [0, k], while the C_2 class consists of the pixels with the values in the range [k+1, L-1]. Then, the probability for the class C_1 will be $p_{1(k)}$.

$$P_1(k) = \sum_{i=0}^{k} p_i \tag{2-4}$$

The probability for the class C_2 will be defined by the equation:

$$P_2(k) = \sum_{k+1}^{L-1} p_i = 1 - P_1(k) \tag{2-5}$$

After that, we calculate the mean intensity value for each class. Therefore, the mean intensity value of the pixels assigned to class C_1 is:

$$m_1(k) = \sum_{i=0}^{k} ip(i/C_i) \tag{2-6}$$

$$= \sum_{i=0}^{k} ip(C_1/i)\, p(i)/p(C_1) = \frac{1}{P_1(k)} \sum_{i=0}^{k} iP_i \tag{2-7}$$

Equation (2-6) indicates that the term $p(i/C_i)$ is the probability of the value i that comes from class C_2. Then, the mean intensity value of the pixels assigned to class C_2 is:

$$\boldsymbol{m_2(k) = \sum_{i=k+1}^{L-1} ip(i/C_2)} \quad (2\text{-}8)$$

$$\boldsymbol{m_2(k)=\frac{1}{P_2\,(k)} \sum_{i=k+1}^{L-1} iP_i} \quad (2\text{-}9)$$

The term $\boldsymbol{p(i/C_2)}$ is the probability of the value i that comes from class $\boldsymbol{C_2}$. Also, the cumulative mean (average intensity) up to level k is given by:

$$\text{m(k)}=\boldsymbol{\sum_{i=0}^{k} i\,P_i} \quad (2\text{-}10)$$

And the global mean which is the average intensity of the entire image is given by:

$$\boldsymbol{m_G}=\boldsymbol{\sum_{i=0}^{L} i\,P_i} \quad (2\text{-}11)$$

The truth of the following two equations (2-12) and (2-13) can be verified by direct substitution of the preceding results:

$$\boldsymbol{P_1\,m_1 + P_2\,m_2 = m_G} \quad (2\text{-}12)$$

And

$$\boldsymbol{P_1 + P_2 = 1} \quad (2\text{-}13)$$

On the other hand, to evaluate the "goodness" of the threshold at level k, we use the normalized dimensionless metric (NDM).

$$\text{NDM} = \frac{\sigma^2{}_B}{\sigma^2{}_G} \quad (2\text{-}14)$$

The global variance ($\boldsymbol{\sigma^2{}_G}$) is the intensity variance of all the pixels in the image, and it is calculated by this equation below:

$$o^2_G = \sum_{i=0}^{l-1} (i - m_G)^2 P_i \quad (2\text{-}15)$$

and o^2_B defines the between- class variance, as given in equation (2-16):

$$o^2_B = P_1 (m_1 - m_G)^2 + P_2 (m_2 - m_G)^2 \quad (2\text{-}16)$$

Also, there is another expression for this term which is given in equation (2-17)

$$o^2_B = \frac{(m_G P_1 - m)^2}{P_1 (1 - P_1)} \quad (2\text{-}17)$$

Therefore, the o^2_B is measure of separability between class, and the larger o^2_B will be indicating a proper thresholding. Also, η is a measure of separability, and maximizing this metric is equivalent to maximizingo^2_B. As a result, the main goal is to determine the threshold value k which maximizes the between- class variance.

As a result, we rewrite the equation (2-14) by reintroducing k and the final result is given in equation (2-18):

$$\text{(k)} = \frac{o^2_B(k)}{o^2_G} \quad (2\text{-}18)$$

and the between- class variance (o^2_B) will be rewritten as in equation (2-19)

$$o^2_B(k) = \frac{(m_G P_1 (\text{k}) - m(k)^2}{P_1 (k)(1 - P_1 (k))} \quad (2\text{-}19)$$

AS a result, the optimum threshold is the value, k^* that maximizes between-class variance (o^2_B):

$$o^2_B(k^*) = \max_{0 \le K \le L-1} o^2_B(k) \quad (2\text{-}20)$$

From this equation, to find $\boldsymbol{k}^*$ we have to evaluate equation (2-20) for all integer values of k and select the value of k that yielded the maximum between- class variance $o^{\boldsymbol{2}}_{\boldsymbol{B}}(\boldsymbol{k})$. After that, when the $\boldsymbol{k}^*$ is obtained, it is considered the optimum threshold value, and the input image f(x,y) is segmented as given in equation (2-21):

$$g(x,y) = \begin{cases} 1 & f(x,y) > k^* \\ 0 & f(x,y) \leq k^* \end{cases} \quad (2\text{-}21)$$

The normalized metric $\boldsymbol{\eta}$ is evaluated at the optimum threshold value, ($\boldsymbol{k}^*$). It is used to estimate the separability of classes, and this measure has values in range of $0 < (\boldsymbol{k}^*) \leq 1$ [20] [27]. Otsu's thresholding method has been adopted instead of the Basic Global Thresholding method due to complication of structures in MRI images.

CHAPTER III

EDGE DETECTION AND COMMON EDGE DETECTION TECHNIQUES USED

3.1 Background (Edge Detection Technique)

Edge detection is a very important technique used in digital image processing. Edge detection can be defined as the process of identifying and locating sharp discontinuities in an image. The discontinuities are abrupt changes in pixel intensity, which characterize boundaries of objects in a scene. Edge detection can be used in many image applications, such as segmentation, registration, identification and recognition; all are based on the edge detection algorithm [28].

There are several ways to model edges. Edge models are classified based on intensity profiles. One of these edge models is a step edge, which involves a transition between two intensity levels occurring ideally over the distance of 1 pixel. Step edges are considered ideal edges. Also, they are used as edge models in algorithm development, such as Canny edge detection which was derived using a step-edge model [20]. On the other hand, when digital images have edges that are blurred and noisy, edges are more closely modeled as having an intensity ramp profile. The slope of the ramp depends on the degree of blurring. As a result, the edge will not be 1 pixel thick because an edge point is any point contained in the ramp. A third model is called roof edge, which contains models of lines through a region, with the base (width) of a roof edge being

determined by the thickness and sharpness of the line. As a result, the performance of edge algorithms will depend on the differences between actual edges and the models used in developing the algorithms [20].

3.2 Other Edge Detection Methods

Ideally, when an edge detector is applied on an image, the result will be an image with a set of connected curves that indicate the boundaries of objects. However, it is not always possible to obtain such ideal edges from real images with moderate complexity [20]. Most known edge detection techniques can be divided into three categories:

- Gradient-Based Methods: gradient-based methods detect edges by searching for maximums and minimums in the first derivative of the image. Sobel, Prewitt, and Robert are examples of gradient-based algorithms [29].
- Laplacian-Based Methods: these methods search for zero-crossings in the second-order derivative expression computed from the image in order to find edges. The Laplacian operator is the most common operator used with zero-crossing method [29].
- Model-Based Methods: there is a wealth of proposed methods, which do not fall into any of the above two categories of methods. They are proposed using different models or algorithms to locate edges from images, and some are very application dependent such as using wavelets [30], fuzzy [31], SVM [32], Cellular Automata [33], and edge detection methods based on Stochastic Entropies or Distances [34].

3.2.1 Gradient-Based Methods (Roberts, Prewitt, Sobel)

An edge can be described by three concepts: edge direction that is perpendicular to the direction of maximum intensity change (i.e., edge normal), edge strength that is related to the local image contrast along the normal, and finally edge position, which is the image position at which the edge is located. So, to find edge strength and direction at location (x,y) of an image f, is the gradient that is denoted by $\boldsymbol{\nabla f}$, and it is defined as the vector [20]:

$$\nabla f \equiv grad(f) \equiv \begin{bmatrix} g_x \\ g_y \end{bmatrix} = \begin{bmatrix} \frac{\partial f}{\partial x} \\ \frac{\partial f}{\partial y} \end{bmatrix} \tag{3-1}$$

The important geometrical property for this vector is points in the direction of the greatest rate of change of f at location (x,y). Also, the magnitude (length) of vector $\boldsymbol{\nabla f}$ is defined as in equation (3-2):

$$\mathrm{M}\ (\mathrm{x}, \mathrm{y}) = mag(\nabla f) = \sqrt{{g^2}_x + {g^2}_y} \tag{3-2}$$

Where mag is the value of the rate of change in the direction of the gradient vector. Also, M (x,y) is images of the same size as the original. Also, x and y are allowed to vary over all pixel locations in f. Therefore, it is common practice to refer to the latter image as the gradient image, or simply as the gradient when the mean is clear [20]. The direction of the gradient vector is defined by the angle as given in equation (3-3):

$$\alpha(x, y) = tan^{-1}\left[\frac{g_y}{g_x}\right] \tag{3-3}$$

This angle is measured with respect to the x-axis. Also, $\boldsymbol{\alpha(x,y)}$ should be an image of the same size as the original image that is created by the array division of image $\boldsymbol{g_y}$ by image $\boldsymbol{g_x}$.

An image requires computing the partial derivatives $\frac{\boldsymbol{\partial f}}{\boldsymbol{\partial x}}$ and $\frac{\boldsymbol{\partial f}}{\boldsymbol{\partial y}}$ at every pixel location in the image to obtain the gradient. It is known that

$$g_x = \frac{\partial f(x,y)}{\partial x} = f(x+1,y) - f(x,y) \tag{3-4}$$

and

$$g_y = \frac{\partial f(x,y)}{\partial y} = f(x,y+1) - f(x,y) \tag{3-5}$$

- Robert's cross operator:

When diagonal edge direction is of interest, it is important to have a 2-D mask. The Roberts cross-gradient operator was one of the first edge detectors and was proposed by Lawrence Roberts in 1965. The Roberts Cross operator performs a simple and quick method to compute a 2-D spatial gradient measurement on an image. The kernels calculate pixel values at each point in the output and represent the estimated absolute magnitude of the spatial gradient of the input image at that point. The operator has a pair

-1	**0**
0	**-1**

G_x

0	**-1**
-1	**0**

G_y

Figure 3-1: Masks Used For Robert's Operator [28].

of 2×2 convolution kernels as shown in Figure 3.1. One kernel is simply the other rotated by 90° [28].

These kernels are designed to respond maximally to edges running at 45° to the pixel grid, one kernel for each of the two perpendicular orientations. The kernels can be applied separately to the input image, to produce separate measurements of the gradient component in each orientation [20]. These can then be combined together to find the absolute magnitude of the gradient at each point and the orientation of that gradient. The gradient magnitude is given by:

$$|G| = \sqrt{G_x + G_y} \tag{3-6}$$

Typically, for faster computations an approximate magnitude is computed using [28].

$$|\,G| = |G_x| + |G_y| \tag{3-7}$$

As a result, 2x2 masks are simple; however, they are not useful for computing edge direction as masks when they are symmetrical about the center point [28].

- Prewitt Operator

The simplest way to present the digital approximation to the partial derivatives can be by using 3x3 masks that are given by:

$$g_x = \frac{\partial f}{\partial x} = (z_7 + z_8 + z_9) - (z_1 + z_2 + z_3) \tag{3-8}$$

and

$$g_y = \frac{\partial f}{\partial y} = (z_3 + z_6 + z_9) - (z_1 + z_4 + z_7) \tag{3-9}$$

These two equations show that the derivative in the x-direction is represented by the difference between the third and the first row of the 3x3 region approximation, while

-1	**-1**	**-1**
0	**0**	**0**
1	**1**	**1**

G_x

-1	**0**	**1**
-1	**0**	**1**
-1	**0**	**1**

G_y

Figure 3-2: Masks Used by Prewitt Operator [28].

the derivation in the y- direction is represented by the difference between the third and the first columns. These approximations are more accurate than the approximations obtained using the Roberts operators. As a result, these two equations can be implemented over an entire image by filtering f with two masks. These two masks are proposed by Prewitt in 1970. Therefore, they are called the Prewitt operators. These masks maximally respond to edges running vertically and horizontally [20] [28].

- Sobel Operators

A pair of 3×3 convolution kernels are used to perform the edge detection process. These kernels or masks are similar to Prewitt operators, but the difference occurred due to a slight variation in the preceding for two equations (3-8, 3-9), which use a weight of 2 in the center coefficient as shown:

$$g_x = \frac{\partial f}{\partial x} = (z_7 + 2z_8 + z_9) - (z_1 + 2z_2 + z_3) \quad (3\text{-}10)$$

and

$$g_y = \frac{\partial f}{\partial y} = (z_3 + 2z_6 + z_9) - (z_1 + 2z_4 + z_7) \quad (3\text{-}11)$$

These masks shown in Figure 3.3 were proposed by Sobel in 1970. These kernels maximally respond to edges running vertically and horizontally relative to the pixel grid, one kernel for each of the two perpendicular orientations. These kernels can be implemented separately to the input image. Each kernel generates separate measurements of the gradient component in each orientation (call these Gx and Gy). To find the absolute magnitude of the gradient for each pixel, equation (3-12) is used.

$$|G| = \sqrt{G_x + G_y} \tag{3-12}$$

Typically, for faster computations an approximate magnitude is computed using equation (3-13) [28].

$$|G| = |G_x| + |G_y| \tag{3-13}$$

As a result, there is a slight computational difference between the Prewitt masks and Sobel masks. However, Sobel operators give better results than Prewitt operators because Sobel masks have better noise-suppression (smoothing) characteristics [28].

-1	**-2**	**-1**
0	**0**	**0**
1	**2**	**1**

G_x

-1	**0**	**-1**
-2	**0**	**-2**
-1	**0**	**-1**

G_y

Figure 3-3: Masks Used by Sobel Operator.

3.2.2 A More Advanced Technique for Edge Detection (Canny Operator)

The canny edge detection algorithm was proposed by Canny in 1986. It is a complex algorithm. However, the Canny edge detection algorithm is considered to be the optimal edge detector [20]. In order to implement the Canny edge detector algorithm, a series of steps must be followed [20] [28].

Step 1:

The first step is to filter out any noise or disruption in the original image before detecting any edges. The easiest way to do so is the Gaussian filter. Once a suitable mask has been calculated, the Gaussian smoothing can be performed using standard convolution methods. The larger the width of the Gaussian mask, the lower is the detector's sensitivity to noise. Also, increasing Gaussian width will result in increasing localization [20].

$$G(x,y) = e^{-\frac{x^2+y^2}{2\sigma^2}} \tag{3-14}$$

where G(x,y) in equation (3-14) denotes the Gaussian function. So, a smoothed image $f_s(x,y)$ is resulted by convolving G and f as shown in equation (3-15):

$$f_s(x,y) = G(x,y) \bigstar \mathrm{f(x,y)} \tag{3-15}$$

Step 2:

The next step is to find the edge strength by taking the gradient of the image. The Sobel operator discussed earlier is used here to perform a 2-D spatial gradient

measurement on an image. Then, the approximate absolute gradient magnitude (edge strength) at each point can be found [28].

Step 3:

The direction of the edge is computed using the gradient in the x and y directions. However, an error will occur when the summation of X is equal to zero. Whenever the gradient in the x direction is equal to zero, the edge direction has to be equal to 90 degrees or 0 degrees, depending on what the value of the gradient in the y-direction is equal to. If GY has a value of zero, the edge direction will equal 0 degrees. Otherwise, the edge direction will equal 90 degrees [28]. Step 4:

Once the edge direction is known, the next step is to relate the edge direction to a direction that can be traced in an image. Therefore, if the pixels of a 5x5 image as shown in Figure 3.4 are aligned follows:

x	**x**	**x**	**x**	**x**
x	**x**	**x**	**x**	**x**
x	**x**	**a**	**x**	**x**
x	**x**	**x**	**x**	**x**
x	**x**	**x**	**x**	**x**

Figure 3-4: Example Shows the Pixels of A 5x5 Image [28].

The four possible directions when describing the surrounding pixels are 0 degrees, 45 degrees, 90 degrees, or 135 degrees. So the edge orientation has to be resolved into one of these four directions depending on which direction it is closest to. Any edge direction falling within the yellow range of (0 to 22.5 & 157.5 to 180 degrees) is set to 0 degrees. Any edge direction falling in the range of (22.5 to 67.5 degrees) is set to 45 degrees. Any edge direction falling in the range of (67.5 to 112.5 degrees) is set to 90 degrees. And finally, any edge direction falling within the range of (112.5 to 157.5 degrees) is set to 135 degrees.

Step 5:

Non-maximum suppression now has to be applied. Non-maximum suppression is used to trace along the edge in the edge direction and set any pixel value that is not considered to be an edge to zero. This will give a thin line in the output image. Non-maximum suppression can be done in several ways, but the core of this approach is by specifying a number of discrete orientations of the edge normal (gradient vector). Therefore, to formulate the non-maximum suppression scheme for a 3x3 region centered at every point (x,y) in $\alpha(x, y)$ one should find the direction d_k that is closest to $\alpha(x, y)$. Then if the value of M(x,y) is less than at least one of the neighbors along d_k let g_N(x,y)=0; otherwise, let g_N(x,y)= M(x,y).Where, g_N(x,y) is the nonmaxima -suppresses image [20] .

Step 6:

Finally, hysteresis is used as a means of eliminating streaking. Streaking is the breaking up of an edge contour caused by the operator output fluctuating above and below the threshold. Using a single threshold T1 and an edge produces an average strength equal to T1, and due to noise, there will be points where the edge dips below the threshold. The edge will be look like a dashed line. To avoid this, hysteresis uses 2 thresholds, a high and a low. Any pixel in the image that has a value greater than T1 is presumed to be an edge pixel, and it is marked as such immediately. Then, any pixels that are connected to this edge pixel and that have a value greater than T2 are also selected as edge pixels [20].

3.2.3 Edge Detection Based on Cellular Automata

3.2.3.1 Introduction

A Cellular Automaton (CA) is an infinite, regular lattice of simple finite state machines that change their states synchronously, according to a local update rule that specifies the new state of each cell based on the old states of its neighbors [33]. The Cellular automata are widely used because the Cellular automata have applications in various fields such as biological models, image processing, language recognition, simulation, computer architecture, cryptography...etc. [33]. Therefore, to introduce a dynamic into the system, it is important to add rules because the "job" of these rules is to define the state of the cells for the next step. Also it is important to define the

neighborhood of the cell because a rule in cellular automata defines the state of a cell as dependent on the neighborhood of the cell.

There are different definitions of neighborhoods possible in cellular automata. Therefore, when a two dimensional lattice is considered, the following definitions are common:

(a) Von Neumann Neighborhood: this includes four cells. The cell above and below, right and left from each cell is called the Von Neumann neighborhood of this cell. Therefore, the radius of this Von Neumann Neighborhood is 1, if only the next layer is considered. Also, the total number of neighbor cells including itself is 5 cells [35].

(b) Moore Neighborhood: this includes eight cells. The Moore neighborhood is considered an enlargement of the von Neumann neighborhood, because it contains the Von Neumann neighborhood and the diagonal cells too. In this case, the radius is also r=1, but the total number of neighbor cells including itself is 9 cells [35].

(c) Extended Moore Neighborhood: it is equivalent to the description of the Moore neighborhood above; however, in this case the neighborhood reaches over the distance of the next adjacent cells. So, the radius of this Extended Moore Neighborhood =2 (or larger). As a result, the total number of neighbor cells including itself is 25 cells [35].

(d) Margolus Neighborhood: it is a completely different approach. It considers 2x2

cells of a lattice at once [35].

Figure 3.5, directly below, shows models of cellular automata neighborhood. The red cell represents the center cell, while the blue cells represent the neighborhood cells. The states of blue cells are used to calculate the next state of the (red) center cell according to the defined rule.

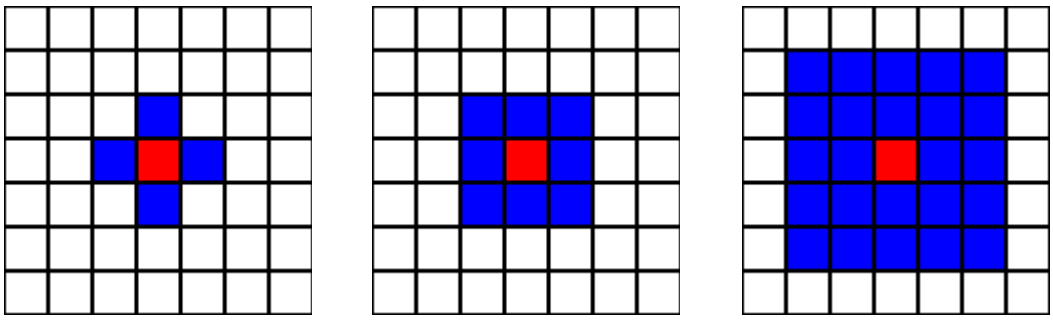

(a)Von Neumann (b)Moore Neighborhood (c) Extended Moore

Figure 3-5: Models of Cellular Automata Neighborhood [35].

3.2.3.2 The Edge Detector Model Based on Cellular Automata

The flowchart in Figure 3.6 shows the steps that should follow for the proposed method of edge detection based on image processing with cellular automata.

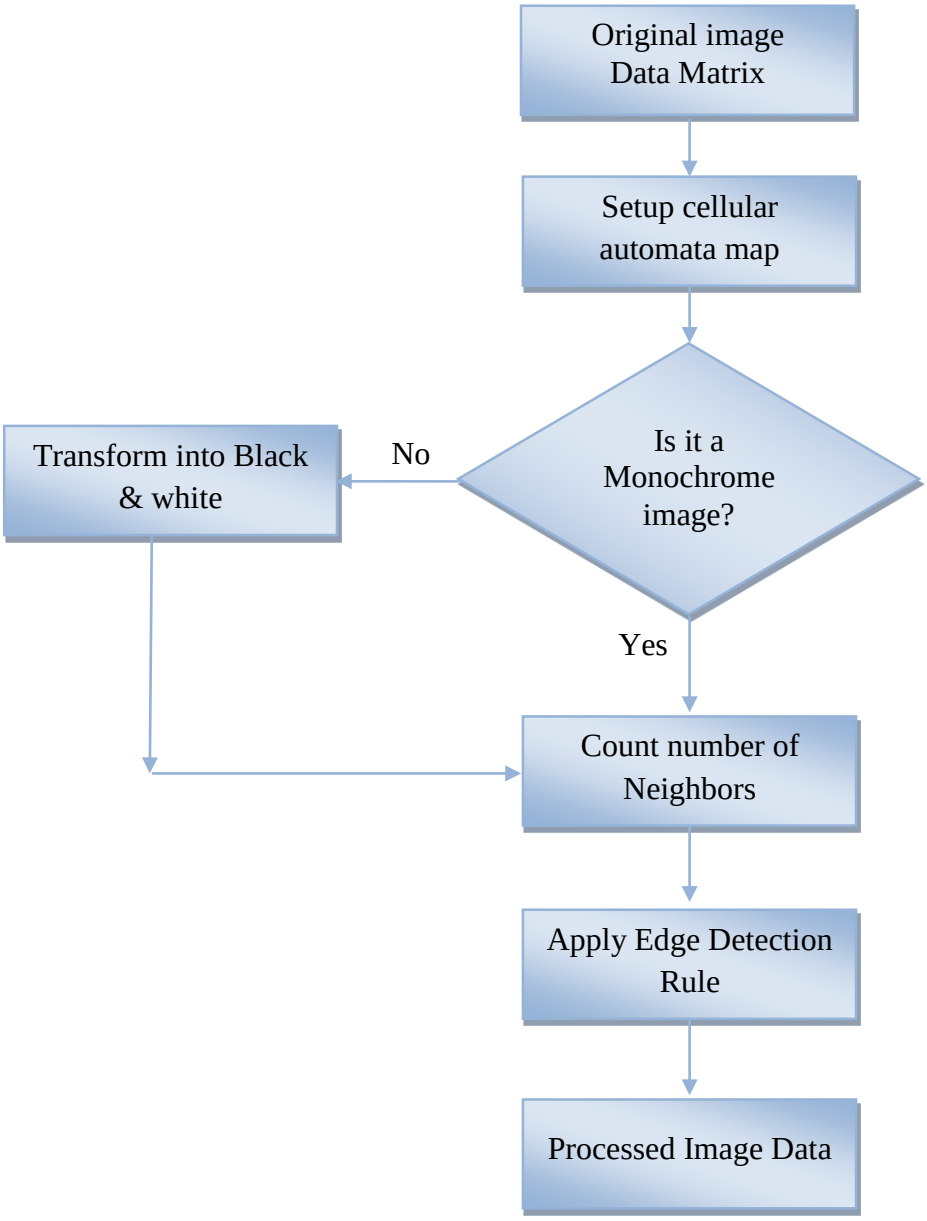

Figure 3-6: Architecture of the Edge Detector Model Based on Cellular Automata.

- In step one, the data information that composes the image is read. As it is known there are different formats of the image (e.g. jpeg, bmp, png, gif, etc.), Therefore, it the format of the image, but all image data should be formed by a data matrix of size M x N [35].
- In step two, the cellular automata map should be set up. The cellular automata map is where the edge detector operation will be performed. It is done by separating each pixel of the original image into one cell directly. Therefore, the image information and the cellular automata map will be composed of a data matrix of the same size of an M x N matrix, thus with MN cells [35].
- In step three, there are different types of images such as color images, gray level images, and pure monochrome (black and white) images. All these images can be processed by this proposed method, but it is necessary to perform black & white transformation before an edge detection operation [35].
- In step four, after applying cellular map of the monochrome image data, the number of neighbors of each cell is counted according to the Moore Neighborhood Model that is the adopted model in this paper [35].
- In step five, an edge detection rule is applied in order to select the characteristics of processing of the image. The next section shows a detailed explanation of the "edge detection rules." In this step, a selection of the cells will be done to detect which cells will die and which will stay alive, and as the result, an edge-detected image is obtained [35].

- In the final step, the result will be a monochrome edge detected image. The size of the processed image (number of columns and rows of the image data matrix) will be exactly the same as that of the original image data [35].

The "Totalistic" Rule is the type of rule employed for edge detection. The state of the next state core cell is only dependent upon the sum of the states of the neighborhood cells, and its own present state. It is important to know that each dead cell has state “0” as value, and each alive cell has a state of “1”. Then, the sum of the states of all the adjacent and diagonal neighbors’ cells is calculated. Therefore, the total number of neighborhood with the central cell is equal to 9. As a result, the sum of the alive neighbor cells can be at maximum 9*1=9. That means all the neighbor cells are alive, while the sum of the dead neighbor will be at the minimum 0*1=0 (all the neighbor cells are dead).

The next step will be applying the "decision rule" that will determine if the cell must become dead or alive. As a result, the total “number of decision rules” is represented by “NDR”, and it is calculated according to the following rubric:

- Number of states: 2. They are 1 for living and 0 for dead.
- Number of neighbors: 10. The number of alive neighbors can be from 0 to 9.
- Thus, NDR = 2 to power 10 = 1024. (Total of 1024 patterns)

1024 patterns is quite a large number of possible rules to be tested. Also, it is necessary to realize that not all the rules are relevant. For example, a rule that kills all the cells could be chosen regardless of the number of alive neighbors, or a rule that keeps all the cells born could be chosen regardless of the number of alive neighbors.

As a result, it is important to select only the rules that present more efficiency for edge detecting of any kind of image. For example, the game of live is when all the cells with 3 alive neighbors or less will die of loneliness, and all the cells with 7 alive neighbors or more will die of over population. Furthermore the cells with 5 alive neighbors will be born, and the cells with 4 or 6 alive neighbors will be born [35]. The decision rule can be interpreted as:

DR = 0 0 0 0 1 1 1 0 0 0.

Therefore, this rule can be redefined as Rule 56 that can be explained by considering the total number of alive neighbors as "NAC", and the next state of the cell will be "NS".

The Moore Neighborhood Model is the model decided upon for use in this thesis because the calculation is applied twice so as to make a clear distinction between pixels where there is a sharp change in intensity [36]. Therefore, NAC can vary from 0 to 9, and NS is "1" or "0" as shown in Figure 3.7:

If NAC = 0 then NS = 0

If NAC = 1 then NS = 0

If NAC = 2 then NS = 0

If NAC = 3 then NS = 0

If NAC = 4 then NS = 1

If NAC = 5 then NS = 1

If NAC = 6 then NS = 1

If NAC = 7 then NS = 0

If NAC = 8 then NS = 0

If NAC = 9 then NS = 0

Figure 3-7: Formulation of Rule 56.

In sum, these traditional edge detection and model based methods such as the cellular automata methods all have advantages and disadvantages, which are summarized in Table 2:

Table 3-1

Summary of Various Edge Detection Methods.

Method	Advantages	Disadvantages
Sobel, Robert	better noise suppression, simple to implement	Discontinuity in edges, Not accurate result
Prewitt	simpler than Sobel	Discontinuity in edges
Canny	Low error rate, Single edge point response	Time consuming, complexity
Cellular Automata	low error rate, continuous edges,	hard to find the suitable rule, Time consuming

It is a fact that there is a need for more efficient methods for detecting edges of a brain tumor that can be used in real time to allow for precise tumor removal and preserve every single normal cell. Therefore, a new technique using Morphological Operations with an erosion process for edge detection is proposed in this work.

CHAPTER IV

PROPOSED FRAMEWORK: EXTRACTION EDGES OF BRAIN TUMOR BY MORPHOLOGICAL OPERATIONS

4.1 Morphological Operations

Mathematical morphology is a tool for extracting image components that are useful in the representation and description of region shape such as boundaries, skeletons, and convex hulls. Also, the morphological techniques are integral for pre- or post-processing such as morphological filtering, thinning, and pruning [20]. Morphological operations are logical transformations based on comparison of pixel neighborhoods with a predetermined pattern. Most morphological operations focus on binary images. Morphological operations offer a unified and powerful approach to numerous image processing needs.

Objects are represented by sets in mathematical morphology. In binary image, the set of all white pixels is a complete morphological description of the image. Therefore, the sets in any equation are members of the 2D integer space E^2 [20]. As a result, each element of the set is a 2-D vector whose coordinates are the (x, y) coordinate of a white or black pixel in the image. The concepts of set reflection and translation are considered the most important concepts in mathematical morphology because they are the primary and most used morphological operations [20].

Reflection is defined by equation (4-1):

$$B^{\wedge} = \{w/w = -b \quad \text{for } b \in B\} \tag{4-1}$$

where $B^{\wedge}$ denotes the reflection of a set B, B is the set of pixels (x,y) representing an object in the image, w is formed by multiplying each of the elements of the set B by -1, and b is an element of B. Hence, $B^{\wedge}$ will be the set of point in B with new coordinates of (-x,-y) [20].

The translation is by equation (4-2):

$$(B)_z = \{C/C = b + z \text{ for } b \in B\} \tag{4-2}$$

where $(B)_z$ denotes the translation of a set B by point $Z = (z_1, z_2)$, and C is formed by translating each of the elements of the set B by z. Thus, $(B)_z$ is the set of points in B whose (x,y) coordinates have been replaced by ($x+z_1$, $y+z_2$) [20].

Reflection and translation are employed extensively in mathematical morphology to formulate operations based on the selected structuring elements (SE_s). This is a small combination of sets or sub images, and it is used to examine an image for properties of interest. There are several examples of structure elements (SE_s) because it can be represented in different shapes according to the object present in the image under consideration [20]. Figure 4.1 shows different examples of structure elements [20].

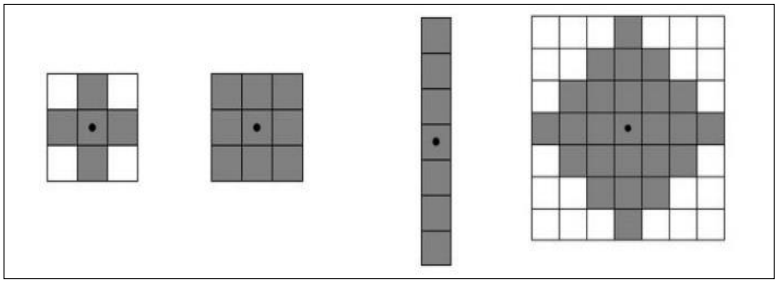

Figure 4-1: Examples of Structure Elements.

Each shaded square in Figure 3.8 denotes a member of the (SE_s). To define which elements are members of SE, the origin of structuring elements have to be specified. Also, the origins of the various SE_s are indicated by a black dot as shown Figure 3.8. The SE_s should consist of rectangular arrays formed by appending the smallest possible number of background elements [20]. The two fundamental morphological operations are: a.) Erosion and b.) Dilation. However, this work used erosion as the focal process.

4.2 Erosion Process

For a binary image, A and B are two sets, in Z^2, eroding the set A by structuring elements of B defined as:

$$(A \Theta B) = \{Z|(B)_z \subseteq A\} \tag{4-3}$$

Equation (3-18) represents the mathematical operation by which erosion occurs. The erosion of A by B is the set of all points Z such that B, translated by Z, is contained in A. Thus, a new set is created by running B over the set A so that the origin of B visits every element of the set A. Therefore, at each location of the origin of the structuring elements of B, if B is completely contained in the set A, we mark the element for that location (where the origin of the structuring element B lays) as a member of the new set.

However, when the origin of the structuring element B is on a border element of the set A, part of B will not be contained in A. Thus, this eliminates the location on which B is centered as a possible member for the new set A. As a result, the boundary of the set is eroded [20].

The specific manner and extent of this shrinking is controlled by the specific shape used as the structuring element [20].

Various shapes have been proposed such as disk, line, octagon, rectangle, and square [20]. A list of parameters is generated to specify needed information other than the shape such as its size. In this proposed algorithm, disk shape has been used as a structuring element, and the accuracy desired necessitates the radius to be 1. Figure 4.2 shows a synthetic example of the Erosion process.

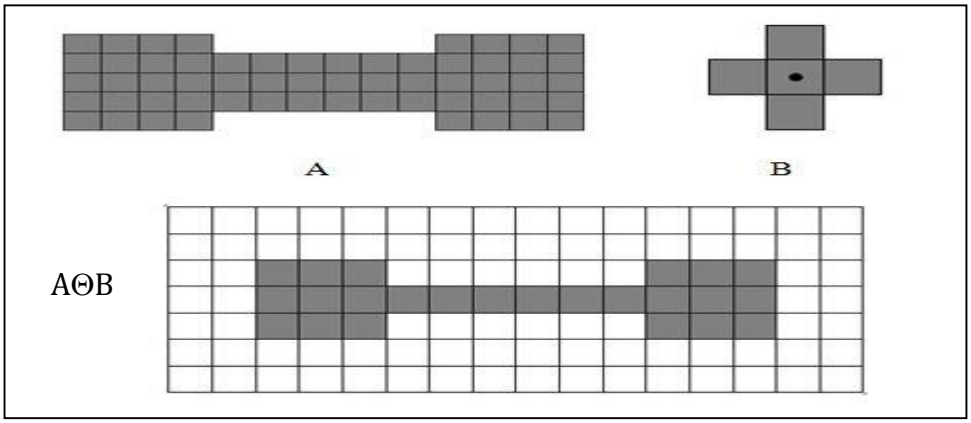

Figure 4-2: Synthetic Example for the Erosion Process.

4.3 Edge Extraction Based Erosion Process

The boundary of a set A can be obtained by first eroding the set A by the structuring element B, and then performing the set difference between A and its erosion. The Boundary of the set A is defined as:

$$\beta(A) = A - (A \Theta B) \tag{4-4}$$

where the boundary of a set A is denoted by $\beta(A)$, and B is the set of suitable structuring elements. Since the size of the structuring elements impacts the thickness for the boundary, this study selected the disk shape structuring elements size of 3×3 to produce a boundary thickness of one pixel. This offers the thinnest possible edges because, for edge detection of tumors, the thin edge is crucial. Figure 4.3 shows a synthetic example of how this algorithm works.

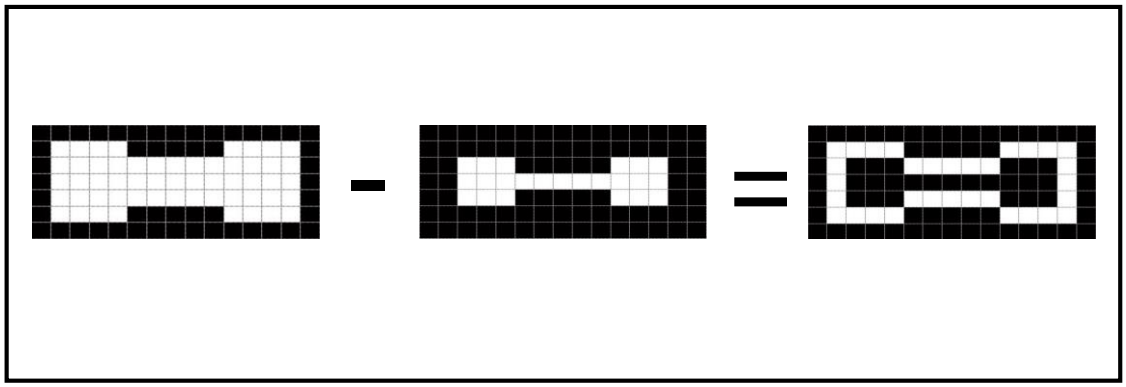

Figure 4-3: Synthetic Example for the Edge Extraction.

CHAPTER V

EXPERIMENTAL RESULTS AND DISCUSSION

To validate the proposed method, it was tested using real data of abnormal images. Numerous Images have been used from The Cancer Imaging Archive (TCIA) [37]. Some of them have been chosen from 130 cases of magnetic resonance (MR) pre-surgical brain tumor patients; including cases of glioblastoma, astrocytomas, and oligodendrogliomas from the REMBRANDT patient population [37]. The others have been chosen from 199 cases of magnetic resonance (MR) from the Cancer Genome Atlas-Low Grade Glioma (TCGA-LGG) patients. All images have the same size pixels region 512X512. These images have different shapes and sizes of brain tumor at different locations within the brain. Dr. Sonia Eden (who is a specialist and neurosurgeon with Borgess Brain & Spine Institute in Kalamazoo) and Dr. Ibrahim al-Mashhadani, (who is a specialist physician in neurosurgery with the Baquba Teaching Hospital in Iraq) were consulted on the diagnosis and recognition of the area of brain tumor and on results. This study also used the same data with the following edge detection methods: Sobel, Prewitt, Robert, Canny, and Cellular Automata. This allowed comparison and evaluation of the method's performance in extraction and detection of a brain tumor.

5.1 Segmentation Process Results

Brain tumor images show a large mass with a surrounding edema. The MR demonstrates the tumor as an area of high signal intensity. In this work, the first step is applying the Segmentation technique using Otsu's thresholding method to extract (or separate) objects that represent a brain tumor from the background. The MATLAB image processing toolbox function im2bw is used. The toolbox function graythresh computes Otsu's threshold. The syntax is:

[T, EM] = graythresh(f)

where T is a threshold that can be used to separate the brain tumor from the background by converting an intensity image to a binary image with im2bw. EM is the effectiveness metric which has a value in the range [0 1]. Its value indicates the effectiveness of the thresholding of the input image. We also present comparison results between Otsu's method and the Global Thresholding method, and midway between black and white (level=0.5, T=127.5) to be able to evaluate Otsu's method performance. We tested these results using the following MR data:

- Figure 5.1 a, on the next page, displays Image 6 (Collection ID: REMBRANDT, Subject ID: 900-00-5346, Series: 7486977714, Number of Images: 80) [37].

Figures 5.1 (b) to 5.1 (d) show the segmented images resulting from using Global, Midway level, and Otsu's method respectively.

As can be seen from figure 4, the Global Thresholding technique gives poor results when trying to segment a tumor because, instead of improving the segmentation results, the entire image components including the tumor portion become distorted in shape. The output obtained using the mid threshold value is inaccurate because it detects the surrounding edema for a brain tumor as a part of a brain tumor area. Otsu's method provides accurate results. Figure 4.1(e) shows the perimeter pixels of brain tumors in the original image to show how the difference between the segmentation of the brain tumor using Otsu's method and the mid threshold value (0.5).

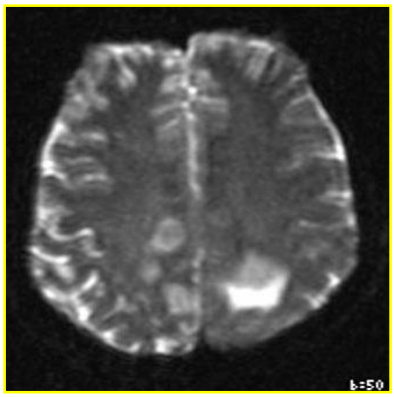

(a) Original Image.

(b) Segmentation by Global Thresholding.

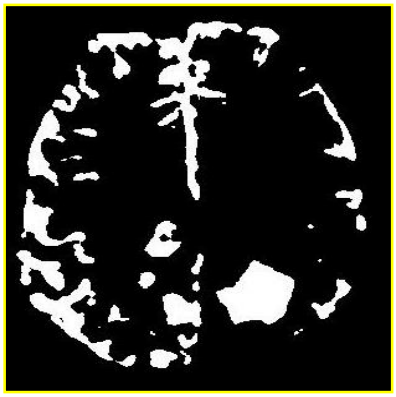

(c) Segmentation by T=0.5.

(d) Segmentation by Otsu's Thresholding.

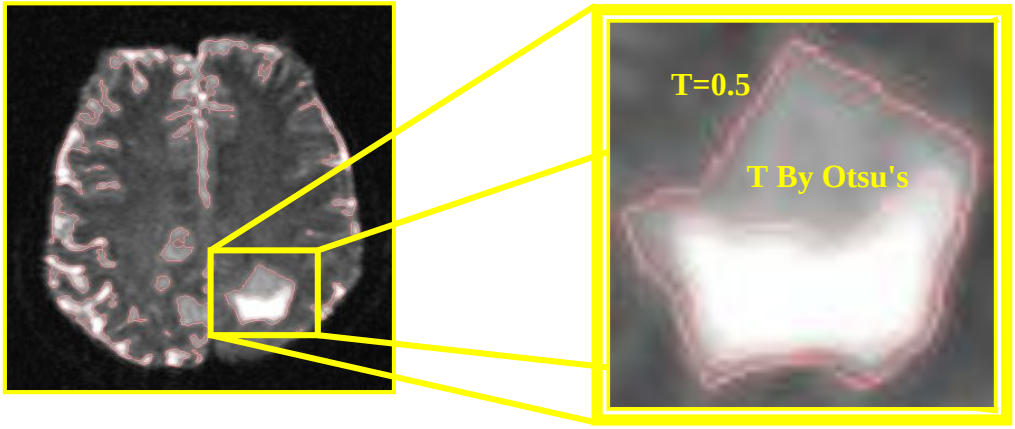

(e) Outline around the Segmented Cell by T=0.5 and Otsu's Thresholding.

Figure 5-1: Segmentation Result for Image 6 (Collection ID: REMBRANDT, Subject ID: 900-00-5346, Series: 7486977714, Number of Images: 80) by Different Thresholding Methods.

5.2 Edge Detection Results

After segmenting the brain tumor area using Otsu's Method, the cropping process has been applied to select the desired area, which is a tumor area. Then, this study's proposed edge detection has been applied. Also, it applies the following edge detection methods: Sobel, Prewitt, Robert, Canny, and Cellular Automata to be able to compare and evaluate this method's performance. The following MRI data has been used:

- Figure 5.2 a, on the next page, displays Image 4 (Collection ID: REMBRANDT, Subject ID: 900-00-5476, Series: 4827408016, Number of Images: 80) [37].

Figure 5.2(b) shows the obtained image after applying Otsu's method. Figure 5.2(c) shows an image after cropping the area of the tumor. Figure 5.2 (d) to Figure 5.2 (i) shows the result after applying Sobel, Robert, Prewitt, Canny, Cellular Automata and the Morphology Operation respectively. As can be seen from Figure 3, the Sobel Operator does not provide exact edges, and shows some edge pixels are missing while it includes false edge pixels. Interestingly, we have similar results with Robert and Prewitt Operators. The Canny operator shows low error, but it also included false edge pixels. Cellular Automata outperforms by providing edges that are two pixels wide; on the other hand, in some regions it also included false edge pixels. The output obtained using Morphological operations based on the Erosion concept shows zero error. Results are free and continuous edges.

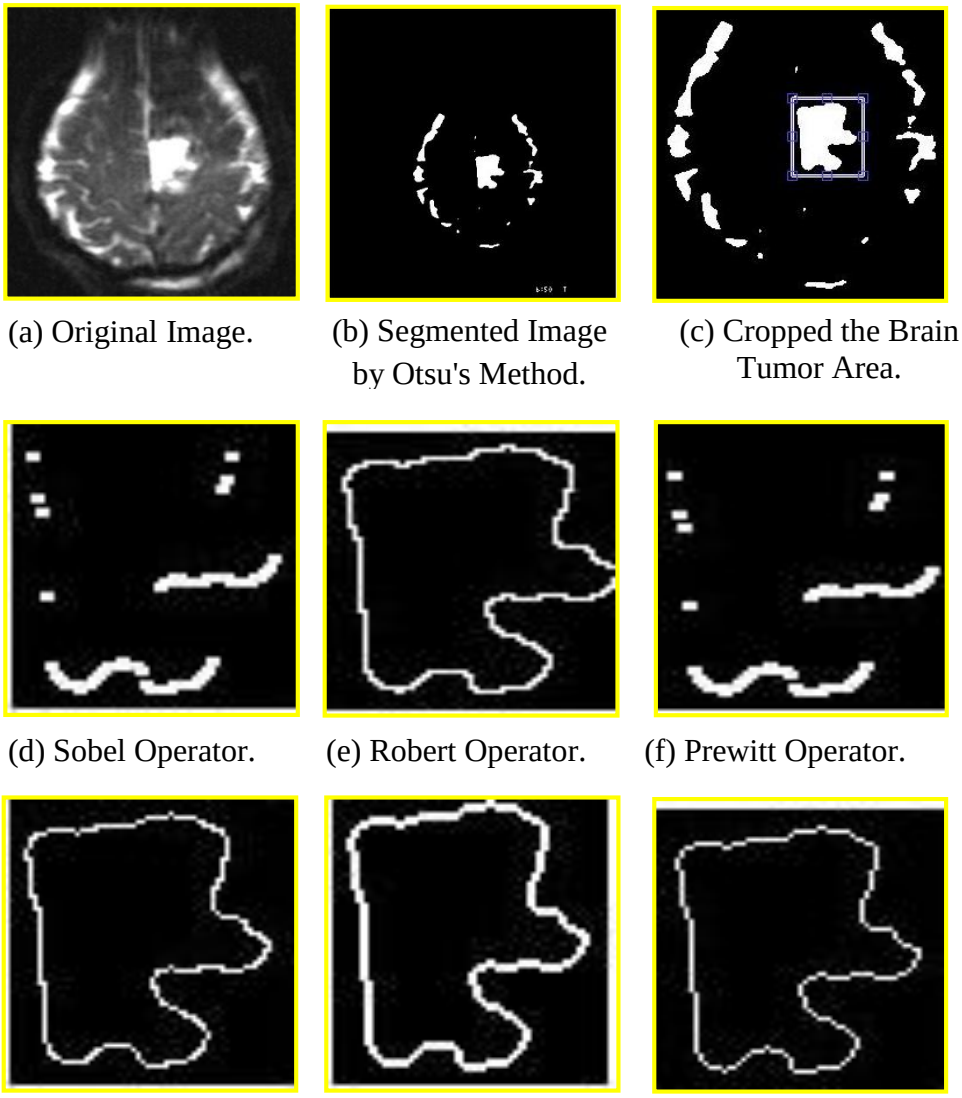

(a) Original Image. (b) Segmented Image by Otsu's Method. (c) Cropped the Brain Tumor Area.

(d) Sobel Operator. (e) Robert Operator. (f) Prewitt Operator.

(g) Canny Operator. (h) Cellular Automata. (i) Morphological Operations.

Figure 5-2: Result for Image 4 (Collection ID: REMBRANDT, Subject ID: 900-00-5476, Series: 4827408016, Number of Images: 80) After Applying Different Edge Detection Method and Our Proposed Method.

Now, to verify these results this study analyzes the result obtained using the Canny operator, Cellular Automata, and Morphological operations based on the Erosion concept method because these results look similar at first glance. The criteria for optimal edge detection has been adopted. This Criteria is defined by three points which are as follows:

1. Good detection: the optimal detector must minimize the probability of false positives (detecting spurious edges caused by noise), as well as that of false negatives (missing real edges). Figure 5.3 (a) shows the true edges for brain tumor area. Figure 5.3 (b) to figure 5.3(d) show the analyzed results for the Canny operator, Cellular Automata, and Morphological operations based on the Erosion concept method respectively. As it can be seen, the Canny operator shows some edge pixels are missing. Cellular Automata and Morphological operations provide continuous edges.

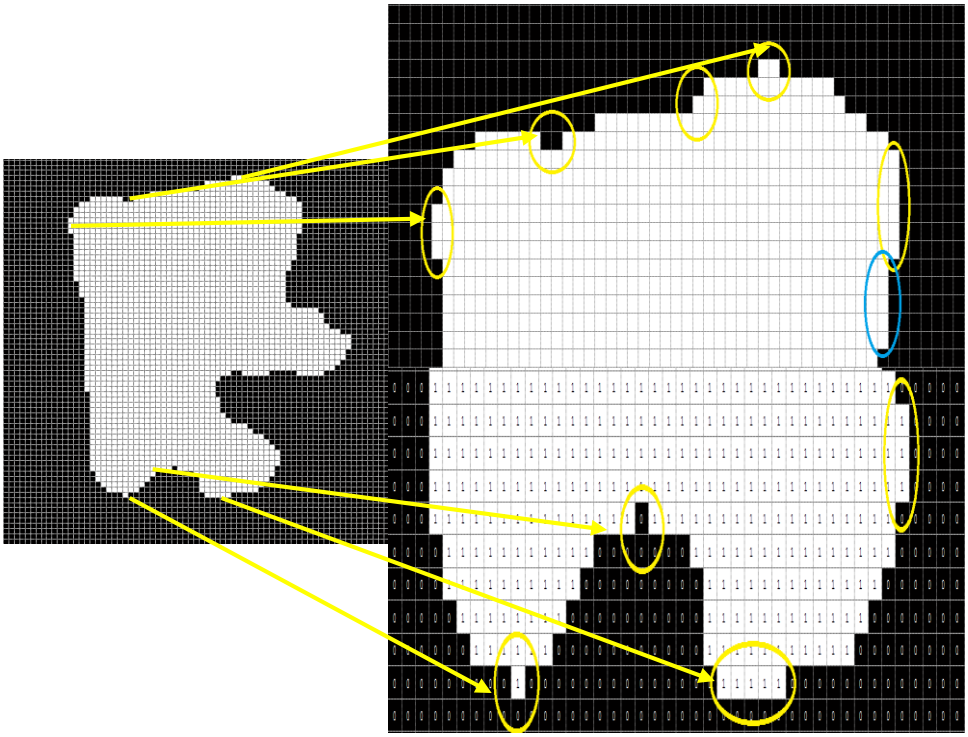

(a) The True Edges for a Brain Tumor Area.

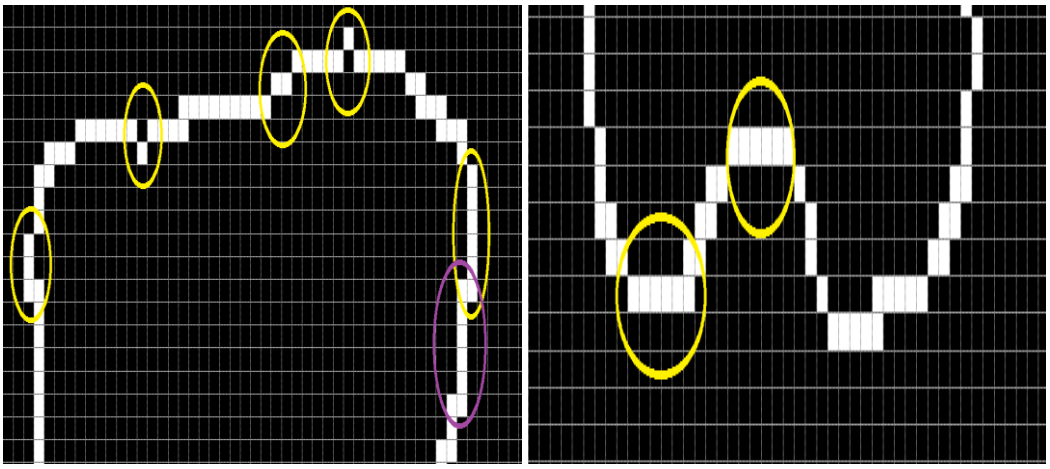

(b) The Brain Tumor Edges Detected by Canny Operator.

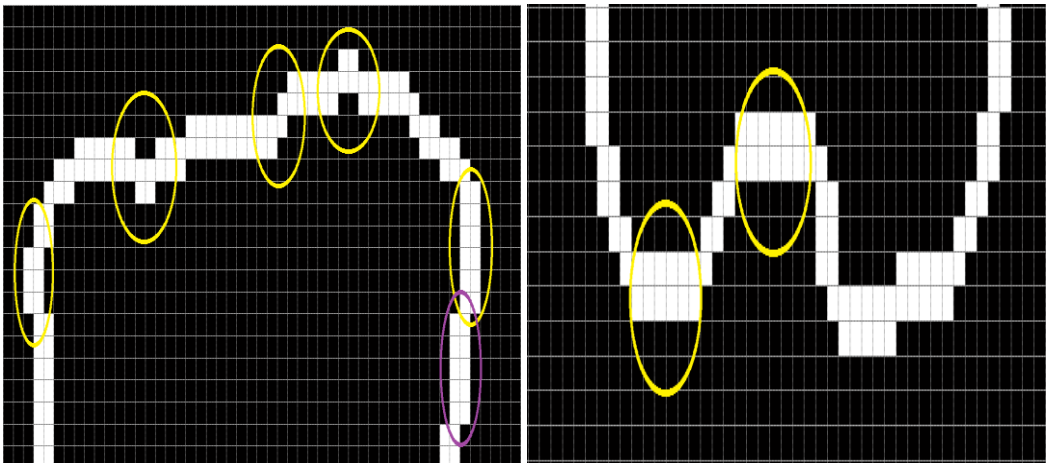

(c) The Brain Tumor Edges Detected by Cellular Automata.

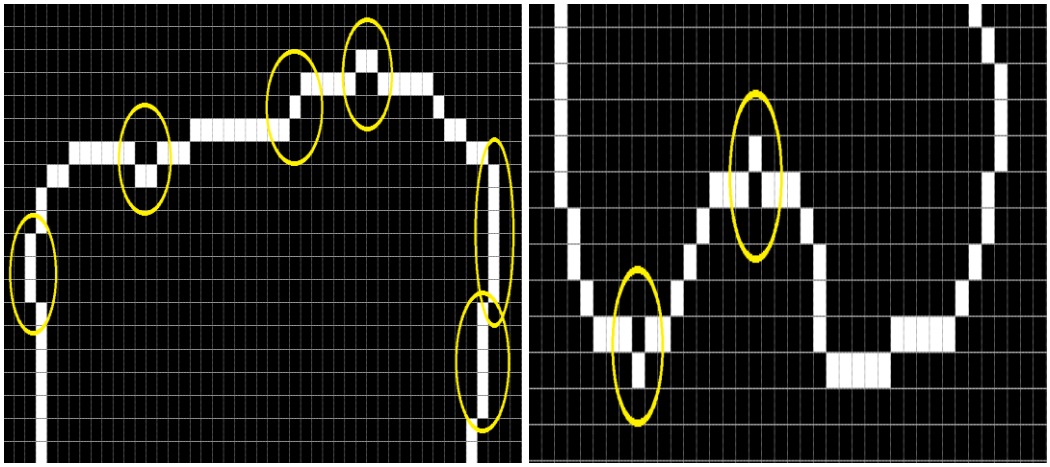

(d) The Brain Tumor Edges Detected by Morphological Operator.

Figure 5-3: Analyzes the Results to Show the Best Detection Method.

2. Localization: is when the edges are detected and must be as close as possible to the true edges. Figure 5.4 (a) shows the true edges for the brain tumor area and their location. Figure 5.4(b) to figure 5.4 (d) show the location of edges obtained by Canny, Cellular Automata, and Morphological operations based on the Erosion concept method respectively. The results show that the Morphological operation is only method that provides exact edge locations.

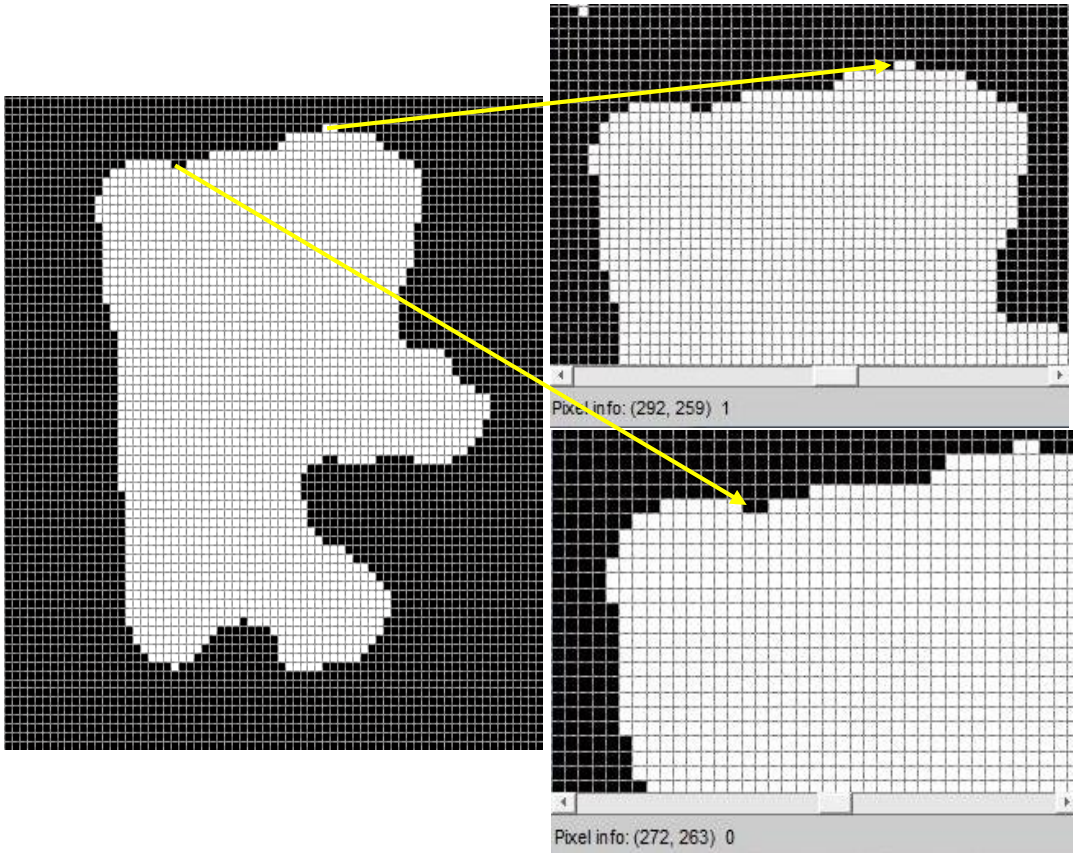

(a) The True Edge Pixels Position for a Brain Tumor.

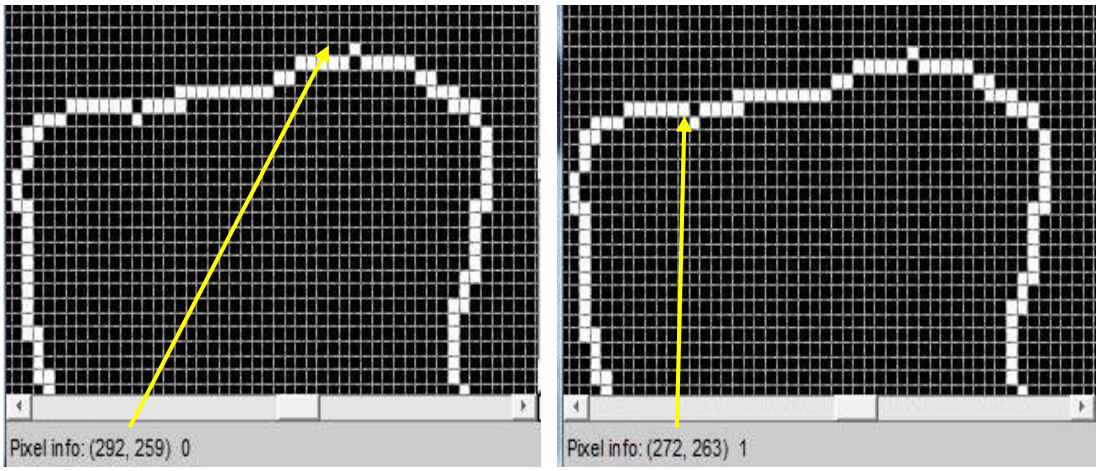

(b) The Brain Tumor Edges Detected by Canny Operator.

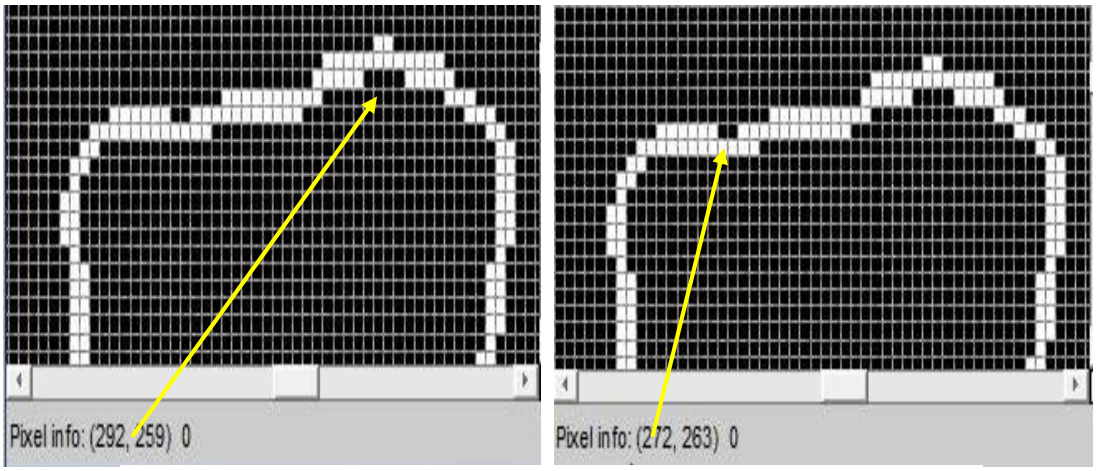

(c) The Brain Tumor Edges Detected by Cellular Automata.

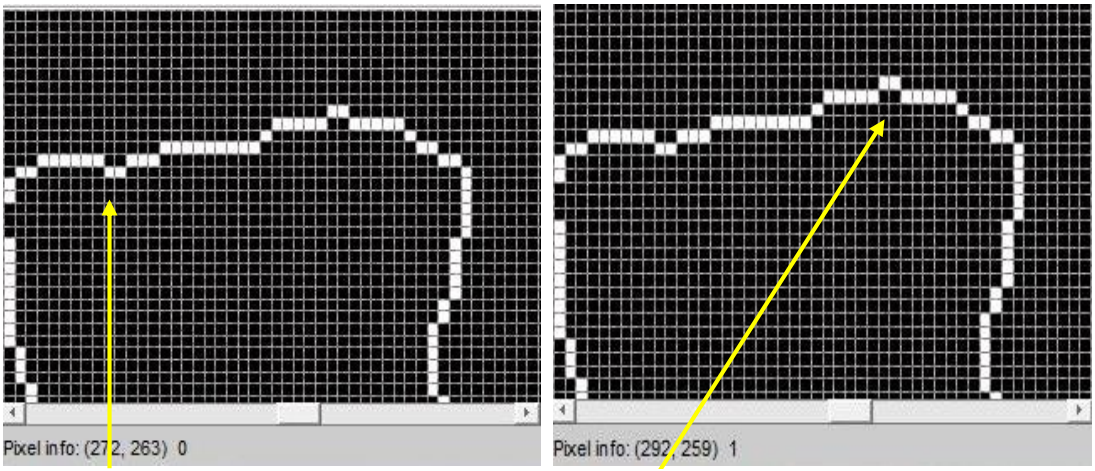

(d) The Brain Tumor Edges Detected by Morphological Operator.

Figure 5-4: Analyzes the Results to Show the Best Localization Method.

3. Single response constraint (thin edges): is when the detector must return one point only for each true edge point. Figure 5.5(a) to Figure 5.5(c) show the measured distance of edges obtained by Canny, Cellular Automata, and Morphological operations based on the Erosion concept method respectively. The results show that Cellular Automata provides two point edges, while Morphological operations and the Canny method provide one point edges.

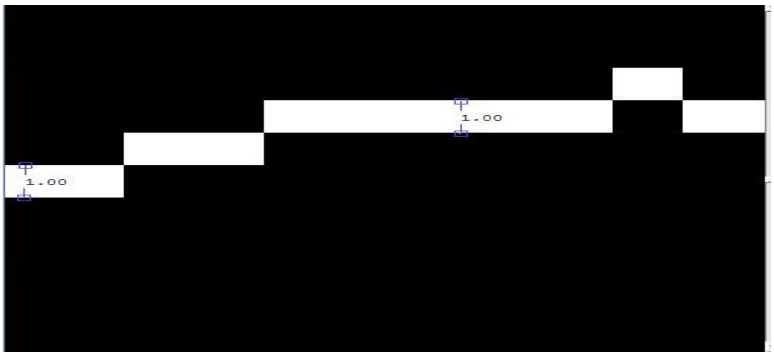

(a) The Thickness of Edges Returned by the Canny Operator.

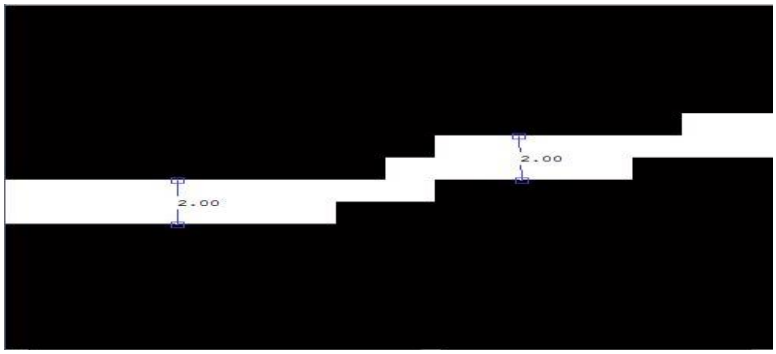

(b) The Thickness of Edges Returned by Cellular Automata.

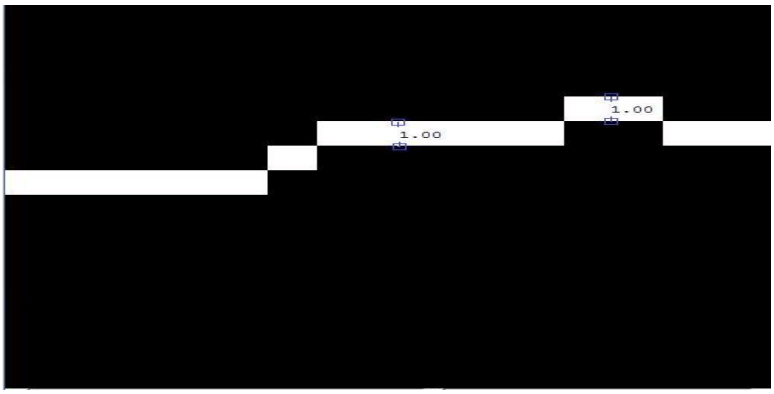

(c) The Thickness of Edges Returned by Morphological Operations.

Figure 5-5: Analyzes the Results to Show the Best Single Response Method.

5.3 The Computational Time Results

The graphs in Figure 5.6 display the time taken by all edge detection methods to produce the boundaries of a brain tumor area. As seen from this study's result, the Cellular Automata edge detection method is the most time consuming method. Time taken by Morphological Operation method is least as compared to other methods.

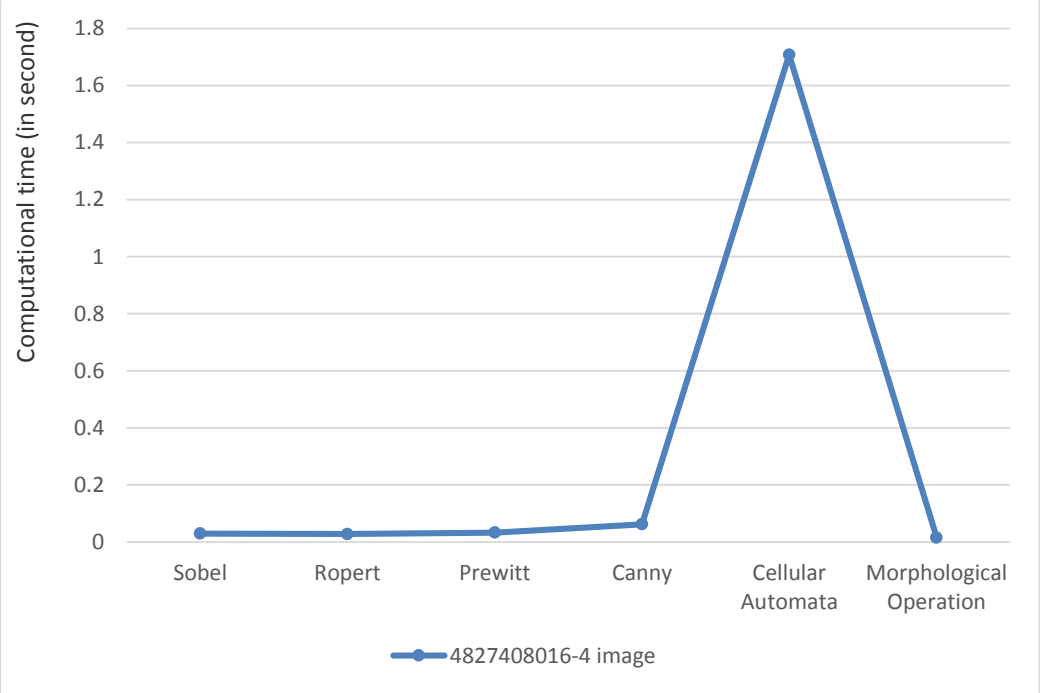

Figure 5-6: Computation Time for Image 4 (Collection ID: REMBRANDT, Subject ID: 900-00-5476, Series: 4827408016, Number of Images: 80 [37]).

CHAPTER VI

CONCLUSION AND FUTURE SCOPE

6.1 Conclusion

This thesis proposed and implemented a new edge detection method using morphological Operators based on the Erosion concept to address the boundary of a brain tumor area. Also, Sobel, Robert, Prewitt, Canny and Cellular Automata edge detection methods have been implemented to allow for a comparison study between this study's proposed method and these methods. As it has been evidenced, this study's proposed method gives exceptional results in terms of accuracy and computation time. The accuracy of the proposed edge detection method is 100%. However, more testing must be conducted to validate the use of this method for detection of tumors on multiple and large databases to affirm the 100% accuracy results.

I would like to propose the following future work possibilities:

1. Conduct more testing to validate the use of this method for detection of tumors in lung , bone cancer, and other types of tumors where the preciseness of tissue edge is paramount

2. An interesting extension of this thesis would be to investigate and quantify the area of the tumor region extracted from other modalities because the doctors are looking for other features for tumors in deferent modalities (such as in CT)

3. This proposed method can be employed to enhance different segmentation methods by combining it with them such as in using other tools such as (Wavelet, K-means, Fuzzy C-means).

REFERENCES

[1] Surgery, American Brain Tumor Association, 2012. Retrieved from http://www.abta.org/secure/surgery.pdf.

[2] About brain tumors: A primer for Patients and Caregivers, American Brain Tumor Association, 2012. Retrieved from http://www.abta.org/secure/about-brain-tumors-a-primer.pdf.

[3] Rachana Rana, H.S Badauria, and Annapurna Singh. "Study of various methods for brain tumor segmentation from MRI images." *International Journal of Emerging Technology and Advanced Engineering*. Vol. 3, Issue 6, June 2013.

[4] Fact Sheet, Central Brain Tumor Registry of the United States (CBTRUS), 2014. Retrieved from http://www.cbtrus.org/factsheet/factsheet.html.

[5] Jolesz, Ferenc A., *Intraoperative Imaging and Image Guided Therapy*, Springer: New York Inc, 2014.

[6] Brain and Spinal Cord Tumor in adults, American Cancer Society, 2014. Retrieved from http://www.cancer.org/acs/groups/cid/documents/webcontent/003088-pdf.pdf.

[7] MRI, National Cancer Institute at the National Institutes of Health. Retrieved from http://www.cancer.gov/dictionary?cdrid=45788.

[8] K.MM. Rao, V.D.P Rao, Medical Image Processing. Retrieved from http://www.drkmm.com/resources/MEDICAL_IMAGE_PROCESSING_25sep06.pdf.

[9] Mamdouh Mahafouz, "Imaging of Brain Tumors," Apr 11, 2013. Retrieved from https://www.youtube.com/watch?v=l2bHrHRefP0.

[10] Mark Schmidt, Automatic Brain Tumor Segmentation, University of Alberta 2005.

[11] Aysha Bava M., and Sifna N. Shajahan, "Segmentation of Brain Tumor in MRI using Multi-structural Element Morphological EdgeDetection," *International Journal of Engineering Research & Technology (IJERT)*, Vol. 3 Issue 3, pp. 313-317, March 2014.

[12] Pratibha Sharma, Manoj Diwakar, and Sangam Choudhary,"Application of Edge Detection for BrainTumor Detection," *International Journal of Computer Applications*, Vol 58, No.16, pp. 21-25, November 2012.

[13] C.C. Leung, W.F. Chen, P.C.K. Kwok, and F.H. Y. Chan, "Brain Tumor Boundary Detection in MR Image with Generalized Fuzzy Operator," *IEEE International Conference on Image Processing*, Vol. 3, pp. II - 1057-60, 14-17 Sept. 2003.

[14] Riries Rulaningtyas, and Khusnul Ain, "Edge Detection For Brain Tumor Pattern Recognition," *IEEE International Conference on Instrumentation, Communications, Information Technology, and Biomedical Engineering (ICICI-BME)*, pp. 1 - 3, 23-25 Nov. 2009.

[15] Manoj Diwakar, Pawan Kumar Patel, and Kunal Gupta, "Cellular Automata Based Edge-Detection For Brain Tumor," *IEEE International Conference on Advances in Computing, Communications and Informatics (ICACCI)*, pp. 53 - 59, 22-25 Aug. 2013.

[16] Nassir Salman, " Image Segmentation and Edge Detection Based on Chas-Vese Algorithm," *The International Arab Journal of Information Technology*, Vol. 3, No. 1, pp. 69-74, January 2006.

[17] S.M. Ali , Loay Kadom Abood , and Rabab Saadoon Abdoon, "Brain Tumor Extraction in MRI Images using Clustering and Morphological Operations Techniques," *International Journal of Geographical Information system Application and Remote Sensing*, Vol. 4, No. 1, pp. 1-14, June 2013.

[18] Hemang J. Shah, "Detection of Tumor in MRI Images using Image Segmentation," *International Journal of Advance Research in Computer Science and Management Studies*, Vol. 2, pp. 53-56, June 2014.

[19] Hemang J. Shah, Hetal Vala, Henita R. Rana, and Zubin Bhaidasna,"Study on Various Methods for Detecting Tumor on MRI Images," *International Journal of Advance Research in Computer Science and Management Studies*, Vol. 2, pp.127-131, February 2014.

[20] Gonzalez, C. R., and Woods, R. E. (2008). Digital Image Processing. Pearson Education International.

[21] Rupali B. Nirgude and Shweta Jain, “Image Enhancement Using Dynamic Region Merging," International Journal of Science and Research (IJSR), Vol. 3, pp.207-211, January 2014.

[22] Gajanayake, G.M.N.R, Yapa, R.D. , and Hewawithana, B., " Comparison of Standard Image Segmentation Methods for Segmentation of Brain Tumors from 2D MR Images," *IEEE International Conference on Industrial and Information Systems (ICIIS),* pp. 301 - 305, 28-31 Dec. 2009.

[23] Rachana Rana, H.S. Bhadauria, and Annapurna Singh, " Comparative Study of Segmentation Techniques for Extracting Brain Tumour from MRI image," *Proceedings of the Second International Conference. on Advances in Electronics, Electrical and Computer Engineering (EEC),* pp. 41-45, 2013.

[24] Ashwini V.Sharma, "Brain Tumor Detection Based On SegmentationUsing Object Labeling Algorithm," *International Journal of Engineering Research & Technology (IJERT),* Vol. 3, pp. 2449-2451, May 2014. Retrieved from http://www.academia.edu/8357208/BrainTumor_Detection_Based_On_Segmentation_Using_Object_Labeling_Algorithm.

[25] Pranita Balaji Kanade, and Prof. P.P. Gumaste,"Brain Tumor Detection Using MRI Images," *International Journal of Innovative Research In Electrical, Electronics, Instrumentation and Control Engineering*, Vol. 3, pp.146-150, February 2015.

[26] Samir Kumar Bandhyopadhyay, and Tuhin Utsab Paul," Segmentation of Brain MRI Image – A Review," *International Journal of Advanced Research in Computer Science and Software Engineering*, Volume 2, pp. 409-413, March 2012.

[27] Tirpude NN, and Welekar RR," Effect of Global Thresholding on Tumor-Bearing Brain Mri Images," *International Journal Of Engineering And Computer Science*, Vol. 2, pp. 728-731, March 2013.

[28] Raman Maini,and Himanshu Aggarwal," Study and Comparison of Various Image Edge Detection Techniques," *International Journal of Image Processing (IJIP),* Vol(3), pp.1-12, 2002. Retrieved from http://wwwmath.tau.ac.il/~turkel/notes/Maini.pdf.

[29] Rashmi, Mukesh Kumar, and Rohini Saxena, "Algorithm and Technique on Various Edge Detection: a survey," *Signal & Image Processing: An International Journal (SIPIJ)* Vol.4, No.3, pp. 65-75, June 2013.

[30] C. Sujathaand and Dr. D. Selvathi, "An Optimal Solution for Image Edge Detection Problem using Simplified Gabor Wavelet," *International Journal of Computer Science, Engineering and Information Technology (IJCSEIT),* Vol. 2, No.3, June 2012.

[31] Abhradita Deepak Borkar, Mithilesh Atulkar, "Detection of Edges using Fuzzy Inference System," *International Journal of Innovative Research in Computer and Communication Engineering* , Vol. 1, Issue1, March 2013.

[32] Sheng Zheng, Jian Liu, and Jin Wen Tian, "A New Efficient SVM-based Edge Detection Method," *Pattern Recognition Letters*, Volume 25 Issue 10, pp. 1143 - 1154, 16 July 2004.

[33] Jarkko Kari, "Cellular Automata: Tutorial" Department of Mathematics, University of Turku, Finland TUCS (Turku Centre for Computer Science).

[34] Abraão D. C. Nascimento, Michelle M. Horta, Alejandro C. Frery, and Renato J. Cintra, "Comparing Edge Detection Methods Based on Stochastic Entropies and Distances for PolSAR Imagery," IEEE Journal of Selected Topics in Applied Earth Observations and Remote Sensing, Vol. 7, Issue 2, pp. 648-663, February, 2014.

[35] Hilton Tamanaha Goi, "An Original Method of Edge Detection Based on Cellular Automata," Department of Electrical Engineering and Computer Science, Korea Advanced Institute of Science and Technology, June 2003.

[36] Manoj Diwakar, Pratibha Sharma, Niranjan Lal, "Edge Detection using Moore Neighborhood," *International Journal of Computer Applications* Vol. 61Issue 3, January 2013.

[37] Clark K, Vendt B, Smith K, Freymann J, Kirby J, Koppel P, Moore S, Phillips S, Maffitt D, Pringle M, Tarbox L, Prior F. "The Cancer Imaging Archive (TCIA): Maintaining and Operating a Public Information Repository." *Journal of Digital Imaging*, Vol. 26, Issue 6,pp.1045-1057, 2013.

APPENDIX

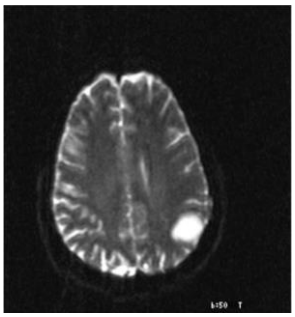

(a) Original Image.

(b) Segmented Image by Otsu's Method.

(c) Cropped the Brain Tumor Area.

(d) Sobel Operator.

(e) Robert Operator.

(f) Prewitt Operator.

(g) Canny Operator.

(h) Cellular Automata.

(i) Morphological Operations.

Result for Image 6 (Collection ID: REMBRANDT, Subject ID: 900-00-5459 Series: 1357990728, Modality: MR,Images: 80) After Applying Different Edge Detection Method and Our Proposed Method.

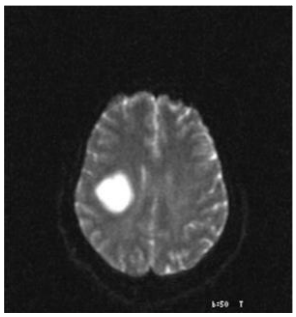

(a) Original Image.

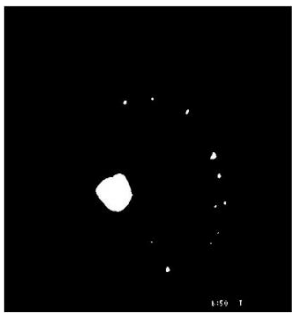

(b) Segmented Image by Otsu's Method.

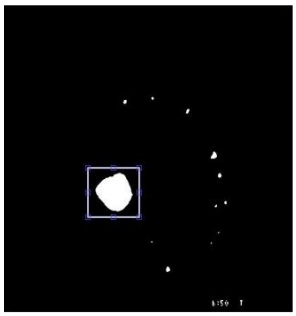

(c) Cropped Brain Tumor Area

(d) Sobel Operator.

(e) Robert Operator.

(f) Prewitt Operator.

(g) Canny Operator.

(h) Cellular Automata.

(i) Morphological Operations.

Result for Image 7 (Collection ID: REMBRANDT, Subject ID: 900-00-1961 Series: 726012900, Modality: MR,Images: 80) After Applying Different Edge Detection Methods and This Study's Proposed Method.

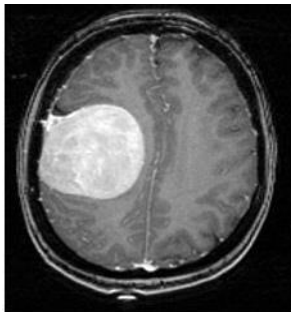

(a) Original Image.

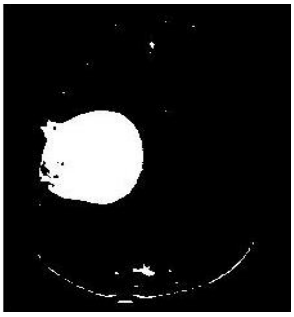

(b) Segmented Image by Otsu's Method.

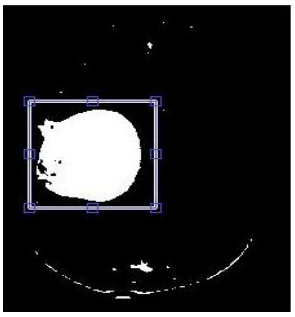

(c) Cropped Brain Tumor Area.

(d) Sobel Operator.

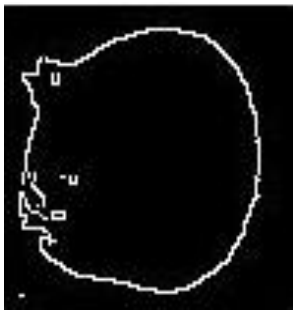

(e) Robert Operator.

(f) Prewitt Operator.

(g) Canny Operator.

(h) Cellular Automata.

(i) Morphological Operations.

Result for Image 7b - Head Film
Http://www.Mc.Vanderbilt.Edu/Documents/Neurosurgery/Images/Headfilm.JPG)
After Applying Different Edge Detection Method and Our Proposed Method.

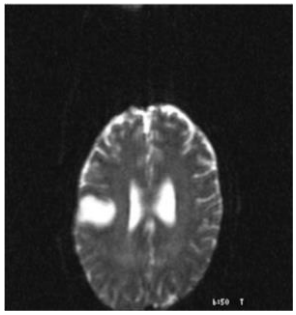

(a) Original Image.

(b) Segmented Image by Otsu's Method.

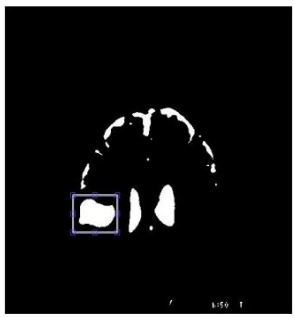

(c) Cropped Brain Tumor Area.

(d) Sobel Operator.

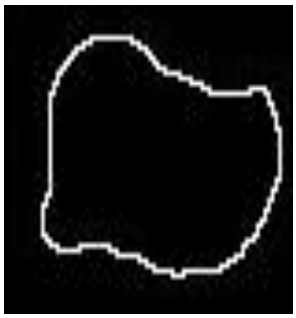

(e) Robert Operator.

(f) Prewitt Operator.

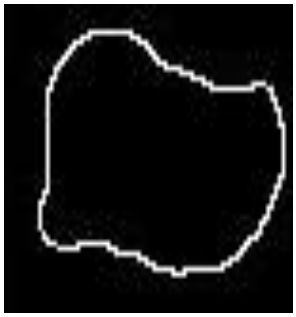

(g) Canny Operator.

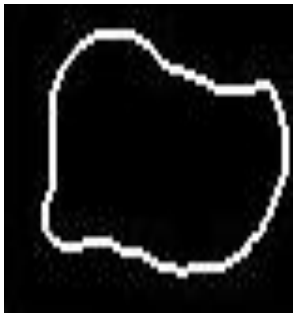

(h) Cellular Automata.

(i) Morphological Operations.

Result for Image 8 (Collection ID: TCGA-LGG(Low Grade Gama), Subject ID: TCGA-CS-5395,Series: 5206190312,Modality:MR,Images:80) [37] After Applying Different Edge Detection Method and Our Proposed Method.

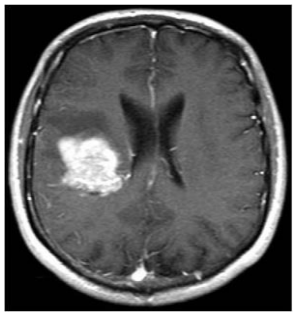

(a) Original Image.

(b) Segmented Image by Otsu's Method.

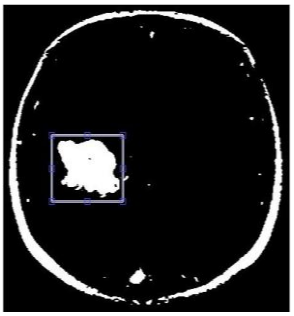

(c) Cropped Brain Tumor Area.

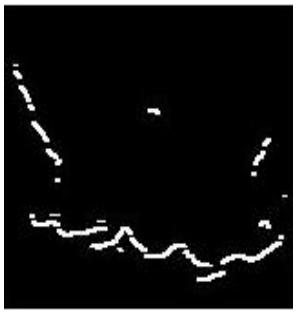

(d) Sobel Operator.

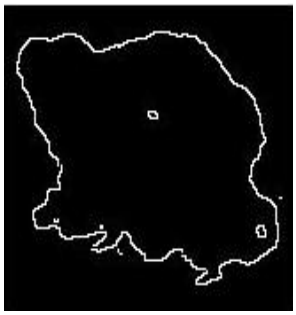

(e) Robert Operator.

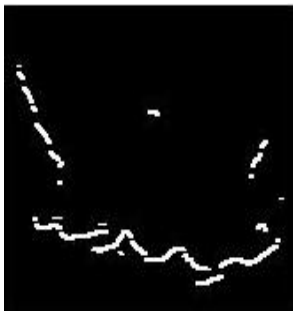

(f) Prewitt Operator.

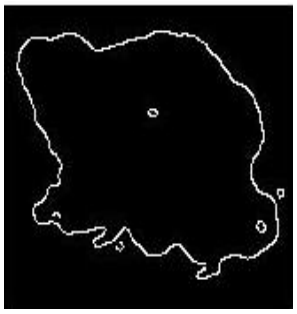

(g) Canny Operator.

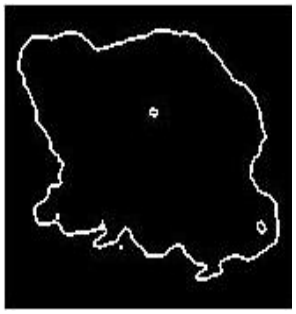

(h) Cellular Automata.

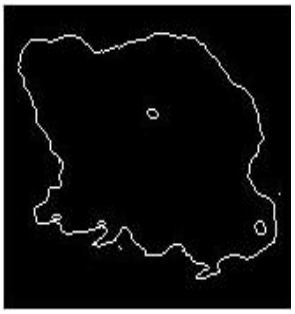

(i) Morphological Operations.

Result for Image Solid Tumor
Http://www.Newswise.Com/Images/Uploads/2009/07/27/Fullsize/Solid_Tumor.Jpg)
After Applying Different Edge Detection Method and Our Proposed Method.